2

The Auditory Nerve: Peripheral Innervation, Cell Body Morphology, and Central Projections

DAVID K. RYUGO

1. Introduction

In mammals, all known auditory information enters the brain by way of the cochlear division of the vestibulocochlear nerve, hereafter referred to as the auditory nerve. Primary neurons, whose cell bodies reside in the spiral ganglion of the cochlea, send peripheral processes out to the organ of Corti to contact the acoustic receptor cells; the central processes or axons bundle together to form the auditory nerve. The terminus of the auditory nerve is the cochlear nucleus. In this way, primary neurons convey the output of the receptors to neurons of the cochlear nucleus. There are two types of receptors, inner hair cells and outer hair cells (Retzius 1884; Ramón y Cajal 1909), two populations of primary neurons (Munzer 1931; Spoendlin 1973), and many neuron classes in the cochlear nucleus (Lorente de Nó 1933; Osen 1969; Brawer, Morest, and Kane 1974). In turn, the cells of the cochlear nucleus give rise to all central auditory pathways. In a general way, the role of the cochlear nucleus is to receive incoming auditory nerve discharges, to preserve or transform the signals, and to distribute outgoing activity to higher brain centers. In order to understand the earliest stages of stimulus coding in the auditory system, we need to know (1) the nature of the signals conveyed by auditory nerve fibers, (2) their source in the periphery, and (3) their destination in the brain. This report shall review the progress that has been made along these lines of investigation.

2. Peripheral Innervation

In mammals, there are four rows of hair cells arrayed longitudinally along the basilar membrane; one row of inner hair cells (IHCs) and three rows of outer hair cells (OHCs). In the cat, there are roughly 3000 IHCs, 9000 OHCs, and 50,000 myelinated axons in the auditory nerve (Retzius 1884; Gacek and Rasmussen 1961); in the mouse, there are 765 IHCs, 2526

OHCs, and 12,350 fibers passing to the organ of Corti (Ehret 1983); and in the rat, there are 960 IHCs, 3470 OHCs, and 15,800 spiral ganglion neurons (Keithley and Feldman 1979, 1982; Berglund and Ryugo 1991). One problem with these quantitative data is that different methods have been used which affect the results. For example, in the cat, the unmyelinated axons were not counted and so they are inferred to number around 2500 based on counts of small ganglion cell bodies (Spoendlin 1971; Kiang et al. 1984). In the mouse, the counts at the habenular openings include both myelinated and unmyelinated primary fibers, but also include the efferent fibers. In humans, there are between 2800–4400 IHCs, 11,200–16,000 OHCs, 31,400 cochlear nerve fibers, and 25,000–30,000 cell bodies in the spiral ganglion (Retzius 1884; Rasmussen 1940; Bredberg 1968). In addition to methodological differences in data collection, there are actual individual variations within a species as well as fundamental variations across species. Quantitative data are nevertheless important because comparative studies in neuronal structure and function can be correlated with life styles of various species. Comparative studies can often provide valuable insight into the behavioral correlates of central nervous system variations (e.g., Irving and Harrison 1967; Masterton et al. 1975).

2.1 Fine Structure of Cochlear Innervation

The nature in which hair cells are connected to the brain will influence how we consider the function of the separate hair cell populations and how we model information passing through the auditory nerve. For example, models of afferent input to the brain will obviously be different if all hair cells receive an identical pattern of innervation or if IHCs have a different innervation pattern than do OHCs. Synapses are located at the base of IHCs and OHCs in the organ of Corti where two types of endings are present (Engström and Wersäll 1958; Kimura 1975; Nadol 1983a,b). One kind of ending contains many round vesicles and is part of the efferent system whose cell bodies reside in the brain stem. The other kind contains few vesicles, exhibits a thickening of its membrane where it apposes the hair cell, and is part of the afferent system whose cell bodies reside in the spiral ganglion.

2.1.1 Inner Hair Cells

There are roughly from 10–30 afferent terminal endings on each IHC in cats (Spoendlin 1969; Liberman 1980a) and a variable number of endings under IHCs of other species (e.g., Nadol 1988a). Moreover, this number appears dependent upon the region of the cochlea sampled (Keithley and Schreiber 1987; Liberman, Dodds, and Pierce 1990). Regardless, the endings of the IHCs are almost exclusively afferent, a conclusion based on

their nonvesiculated appearance and their abutment against synaptic bodies of the hair cell (Kimura 1975). Each small afferent ending typically forms a single synapse with the hair cell (Spoendlin 1973; Liberman 1980a). At the synapse, the plasma membranes of the afferent terminal and hair cell are separated by a narrow gap (100–150 Å) and the afferent terminal membrane bears a dense, fuzzy coat (Fig. 2.1). The region of membrane bearing this coat as reconstructed from serial sections would appear as an elliptical plate (dimensions roughly 0.7 × 0.5 μm). Within the hair cell cytoplasm, positioned along a groove in the presynaptic membrane, is found the synaptic body around which is clustered round vesicles, approximately 35 nm in diameter. The synaptic body is an electron-dense, elongated structure oriented parallel to the long axis of the synaptic plate. Synaptic bodies range in length from 0.2–0.6 μm and 0.06–0.12 μm in diameter. The endings originate from radial fibers of the spiral ganglion which pass through the habenular openings to reach the base of the IHC (Smith 1961; Spoendlin 1973; Liberman 1980a). Radial fibers

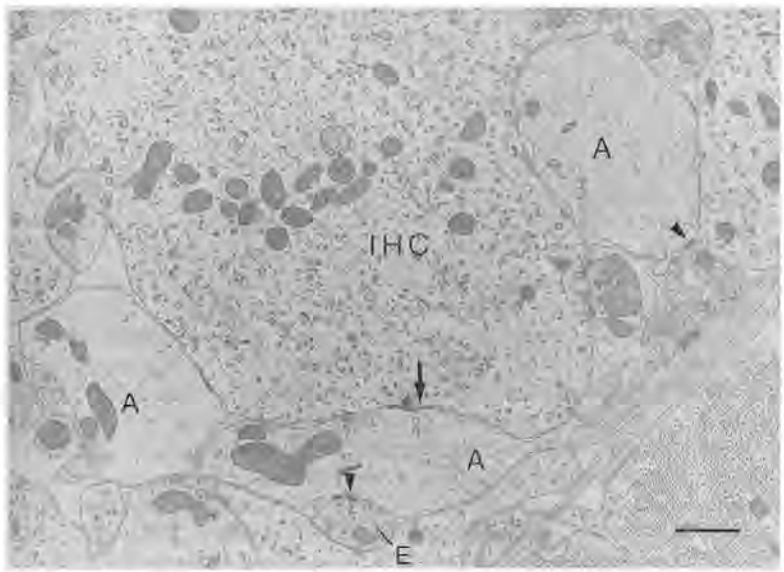

FIGURE 2.1. Afferent nerve endings (A) near the base of an IHC in a squirrel monkey. One afferent ending receives a synapse (arrow) characterized by a marked thickening of the postsynaptic membrane and a presynaptic body surrounded by a halo of round vesicles. An efferent ending (E), filled with synaptic vesicles, forms a synapse (arrowhead) on the afferent ending. Efferent endings do not usually make synaptic contact directly with the IHC. Scale bar equals 1 μm. (This micrograph is courtesy of Dr. R.S. Kimura.)

in the mature cat rarely if ever branch (Spoendlin 1973; Liberman 1980a, 1982a,b), but if they do, they are restricted to the region apical to the 1 kHz point (Liberman, Dodds, and Pierce 1990). Consequently, individual type I spiral ganglion neurons tend to receive all of their input from a single IHC. A single IHC, however, is divergent in that it sends information to the brain by way of many type I neurons, and each type I neuron makes synaptic contact with many different cell types in the cochlear nucleus.

Vesiculated endings do not usually make direct contact with IHCs. Instead, they establish what appears to be a typical axodendritic synapse on the afferent process postsynaptic to the hair cell (Smith 1961; Smith and Rasmussen 1963; Liberman 1980b). In the basal half of the cochlea, each radial fiber received approximately 30 efferent synapses, whereas in the apical half, there were from 35–40 efferent synapses per radial fiber (Liberman, Dodds, and Pierce 1990). These efferents belong to what is commonly called the lateral olivocochlear system (Warr and Guinan 1979; Guinan, Warr, and Norris 1983; White and Warr 1983). The cell bodies of these efferents are relatively small and fusiform in shape, stain positively for the presence of acetylcholinesterase, and lie within the superior olivary complex, lateral to the medial superior olive (Warr 1975). The axons of the lateral olivocochlear efferents are thin and unmyelinated (Brown et al. 1988b).

2.1.2 Outer Hair Cells

There are two types of endings under OHCs. Small, nonvesiculated endings are considered to be afferent and large, vesiculated endings are considered to be efferent. In the cat, there are between 4 and 10 afferent terminal endings under each OHC in the cochlear base (20–50 kHz region) and this number gradually increases to about 10–20 afferent endings under each OHC in the cochlear apex (below 3 kHz region; Simmons and Liberman 1988; Liberman, Dodds, and Pierce 1990). At the synapse, the width of the hair cell membrane tends to be slightly thicker than that of the afferent terminal, separated by a gap of approximately 150 Å (Fig. 2.2). In 30–40% of the cases, a synaptic body is present but variable in size and shape and surrounded by a few vesicles; in the remaining cases, no synaptic body is observed (Dunn 1975; Nadol 1983b). These afferent endings are typically surrounded by vesiculated endings and are sometimes postsynaptic to them (Kimura 1975). Because individual outer spiral fibers can emit up to 60 terminal endings (Simmons and Liberman 1988), a single type II spiral ganglion neuron receives converging inputs from many OHCs, and a single OHC sends its information to the brain by way of a small but variable number of type II neurons. In contrast to the innervation density observed under IHCs, the number of afferent terminals per OHC tends to fall from apex to base (Liberman, Dodds, and Pierce 1990).

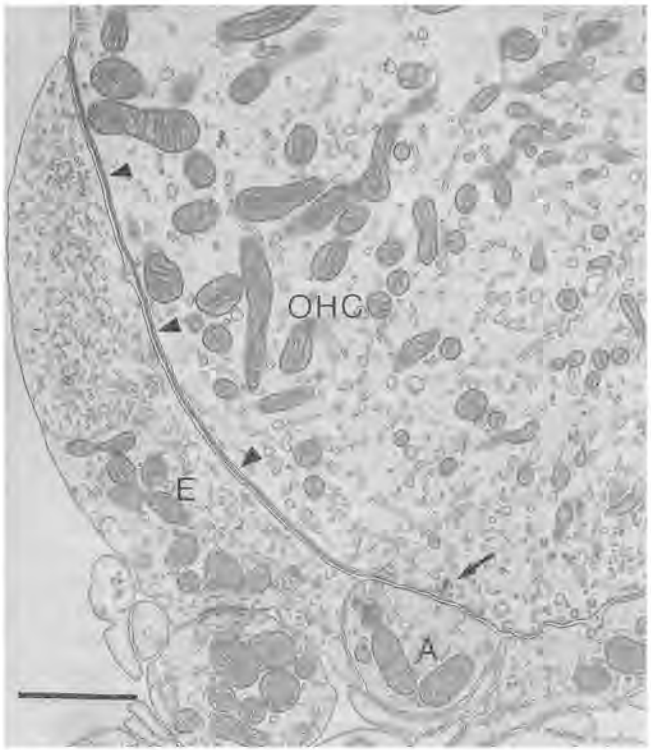

FIGURE 2.2. Nerve endings at the base of an OHC of a rhesus monkey. The afferent nerve ending (A) is relatively small and the synaptic contact with the hair cell (arrow) is characterized by a membrane thickening, a presynaptic body, and a few synaptic vesicles. The efferent ending (E) is typically large, filled with synaptic vesicles, and makes direct contact with the outer hair cell. In addition to the synaptic vesicles, the efferent ending opposes a long subsynaptic cystern (arrowheads) inside the hair cell. Scale bar equals 1 μm. (This micrograph is courtesy of Dr. R.S. Kimura.)

Efferent endings are typically larger (3 μm in diameter) than the afferent endings (1 μm) and they generally make direct contact with the hair cell (Smith and Sjöstrand 1961; Spoendlin 1969; Kimura 1975; Nadol 1983b). The membrane appositions between efferent terminals and OHC are smooth with patches of electron-dense material appearing along the presynaptic membrane. The membranes on both sides of the synaptic gap are equal in thickness and the synaptic gap (approximately 190 Å) is slightly larger than those of the afferent endings. These efferent endings are from the so-called medial olivocochlear system and have thick mye-

linated axons (Brown 1987b; Brown et al. 1988b). The larger cell bodies of the superior olivary complex, located medial to the medial superior olive, give rise to these thick efferent axons (Warr and Guinan 1979; Guinan, Warr, and Norris 1983; White and Warr 1983). Efferent innervation of OHCs becomes less frequent in the apical regions of the cochlea (Smith 1961; Ishii and Balough 1968; Guinan, Warr, and Norris 1983; Liberman, Dodds, and Pierce 1990) and the size of the efferent boutons becomes smaller (Brown 1987b).

Medial olivocochlear efferent fibers (but not lateral olivocochlear efferent fibers) in mouse, gerbil, and cat have been shown to send collaterals to the granule cell regions of the cochlear nucleus ipsilateral to their cochlear target (Brown et al. 1988b). These observations are based on the horseradish peroxidase (HRP) method that permits the continuous tracing of individually stained axons. The time-consuming and technically demanding reconstructions required of this method, however, make it difficult to have a large sample size. Nevertheless, these single fiber data are consistent with retrograde labeling studies, where labeled cell bodies of efferent neurons were never (Covey, Jones, and Casseday 1984; Spangler et al. 1987) or rarely (Adams 1983) found in regions known to be the origins of the lateral efferent system, whereas many labeled somata were found associated with the medial efferent system following tracer injections in the cochlear nucleus. Unfortunately, one study using an alternative population method in the gerbil reached a somewhat different conclusion (Ryan et al. 1987). Following cochlear incubation with D[^{3}H]aspartic acid and subsequent autoradiographic processing, lateral (but not medial) somata were labeled in the brain stem and labeled fibers were seen entering the cochlear nucleus where they terminated in the central part of the ventral cochlear nucleus, a region where no HRP-labeled olivocochlear efferents were observed. Ryan et al. (1987) concluded that fibers of the lateral efferent system branched to innervate the cochlear nucleus. This conflict is resolvable if there exists a subpopulation of efferents from the lateral system that are not revealed using HRP methods.

The differential distribution of efferent endings along the cochlear spiral implies that the system will have less "feedback" influence on afferent information originating from more apical regions, where low frequencies are encoded. Electrophysiological data are consistent with this idea (Wiederhold 1970). When electrical shocks are applied to the olivocochlear bundle, sound-evoked responses of IHCs (Brown and Nuttall 1984) and type I afferents (Wiederhold and Kiang 1970) are reduced, presumably due to activation of the medial olivocochlear efferents (Gifford and Guinan 1987). The idea is that the thick, myelinated medial efferents have much lower thresholds and greater ability to follow the high-frequency shock rates than do the thin, unmyelinated lateral efferents. Because the medial efferents project to the OHCs and the affected neural

responses are from type I afferents innervating IHCs, efferent modification of the OHCs is hypothesized to be mechanically coupled to the IHCs, thereby altering IHC output (Brown and Nuttall 1984; Kiang et al. 1986). This altered receptor output is then reflected in the responses of the type I auditory nerve fibers.

2.1.3 Human Cochlear Anatomy

The fundamental structural plan of the mammalian cochlea is remarkably similar across species. Although there are some differences when comparing humans to other mammals, the functional significance of these differences remains to be determined. The afferent innervation density for both IHCs and OHCs is somewhat lower in humans than what has been found in other mammals, such as guinea pig and cat (Nadol 1988a,b). There are roughly 10 afferent endings per IHC throughout the cochlear length, but for OHCs, the number is four per OHC in the base and rises to eight per OHC in the apex. Furthermore, it is common for a single radial fiber to branch and innervate up to three adjacent IHCs, and for an IHC to form multiple synapses with a single afferent terminal (Nadol 1983a). This situation is different from the unbranched, single synapse afferents in the cat (Spoendlin 1973; Liberman 1980a), but the functional significance of such differences is not known. In addition, there is evidence for reciprocal synapses under OHCs in humans (Nadol 1981, 1983b). That is, some afferent terminals demonstrate synaptic specializations consistent with transmission from neuron to hair cell. Since a single outer spiral fiber contacts many OHCs along a segment of cochlea, reciprocal synapses may be a mechanism whereby one OHC could affect the output of nearby OHCs in surrounding frequency regions. The result might produce a kind of "lateral inhibition" for sharpening frequency resolution.

2.2 Innervation Density

In order to understand the possible substrate for hearing sensitivity, the relationship between sensory receptor density, receptor innervation density, and frequency sensitivity has been investigated. Variations are present in the number of IHCs and OHCs per mm along the organ of Corti (Ehret and Frankenreiter 1977; Ramprashad et al. 1978; Bruns and Schmieszek 1980; Bohne, Kenworthy, and Carr 1982; Liberman 1982b; Burda 1984) and in hair cell innervation density (Spoendlin 1972; Morrison, Schindler, and Wersäll 1975; Nadol 1983a,b; Keithley and Schreiber 1987). An average number of type I afferent terminals per IHC can be calculated based on figures published. The number is 8–11 for human (Held 1926; Guild et al. 1931; Nadol 1988a), 10 for guinea pig (Firbas 1972), 13 for mouse (Ehret and Frankenreiter 1977; Ehret 1979; Keithley

and Feldman 1983), 10–26 for cat (Gacek and Rasmussen 1961; Spoendlin 1969, 1973; Liberman 1980a; Keithley and Schreiber 1987; Liberman, Dodds, and Pierce 1990), 8–24 for horseshoe bat (Bruns and Schmieszek 1980), and 70 for the little brown bat (Ramprashad et al. 1978). Innervation density, however, is not homogeneous along the cochlear length. In the cat, for example, innervation density rises progressively from 10 per IHC in the apex to approximately 30 per IHC in the base (Keithley and Schreiber 1987; Liberman, Dodds, and Pierce 1990).

Significantly less is known about afferent innervation density for OHCs, an issue complicated by the amount of outer spiral fiber branching (Smith 1975). Published counts of innervation density per single OHC yield 7–10 for man (Held 1926), 5–15 for guinea pig (Smith and Sjöstrand 1961), 6–10 for cat (Spoendlin 1969), and 3 for horseshoe bat (Bruns and Schmieszek 1980). The variation in the number of afferent terminals per OHC also differs with respect to the row in which the OHC resides (Liberman, Dodds, and Pierce 1990). With the exception of the little brown bat, fluctuations of innervation density across the above-mentioned mammals seems relatively minor and may not have any significant effect on auditory function. Within a species, however, absolute threshold sensitivity tends to correspond with frequency regions having the highest inner and outer hair cell density and the highest nerve fiber density (Ramprashad et al. 1979; Ehret 1983). It is a working hypothesis that by considering structural variations in the context of acoustic requirements and behavioral adaptations of individual species, we may gain insight into those structural features that contribute to specific features of auditory function.

Since the audiogram for the population of single auditory nerve fibers is similar to the behavioral audiogram in cats (Liberman and Kiang 1978), behavioral thresholds might possibly be explainable at the level of single primary neurons, since an animal should not be more sensitive than its basic units. A different role for hair cell and/or innervation density could be proposed whereby frequency discrimination is the result of variations in receptor density per octave. One part to this argument is derived from the observation that in the cochlea of the greater horseshoe bat, there is a widely expanded frequency representation between 83 and 83.2 kHz creating an "acoustic fovea" (Bruns and Schmieszek 1980). This behaviorally important frequency range is the constant frequency segment of the bat's signal used to echolocate moving prey. The other part of the argument arises by analyzing the number of IHCs per octave and comparing discrimination sensitivity. Between the 1 and 2 kHz region of the cochlea, humans have roughly 360 IHCs, whereas cats have 270 IHCs; within this range of hearing, humans are better at making frequency discriminations (Schuknecht 1960; Liberman 1982b; Nadol 1983a; Fay 1988).

2.3 *Ganglion Cells and Hair Cell Innervation*

The studies described so far have limited their analyses primarily to the organ of Corti. The examination of restricted regions is obviously easier than that of large regions. This research "strategy" is highly practical when studying primary auditory neurons because the cell bodies and peripheral processes are encased in the bony capsule of the cochlea and the central processes terminate several millimeters away in the brain. This situation leads to nontrivial technical problems in the study of cochlear neurons because bone must be removed or decalcified in order to access the cochlear tissue. The histological preparation of bone using calcium chelating agents (e.g., dilute hydrochloric acid or ethylenediamine tetraacetic acid) can compromise cochlear tissue if adequate care is not taken to preserve the tissue while simultaneously decalcifying the bone. Another technical obstacle in studying primary neurons (and in fact all neurons) is that no single staining procedure reveals all aspects of a neuron. For example, Nissl stains reveal ribosomes and chromatin material, and so provide cytological details of the cell body and nucleus but not of the processes (ribosomes and chromatin are not present in dendrites or axons). Protargol, a proteinaceous silver compound, presumably condenses neurofilaments into neurofibrils, thereby revealing the skeletal form of the cell body and its processes (Gray and Guillery 1966). The Golgi method randomly stains individual neurons in their entirety (except for the myelinated axons) by way of a silver or mercuric chromate precipitate, but obscures all internal features (Ramón-Moliner 1970; Valverde 1970). Thus, an image of primary auditory neurons has historically been formed by combining observations from different staining procedures, sometimes from different species, and often from animals of different ages.

The classic descriptions of primary auditory neurons were based on the Golgi method applied to neonatal mice and cats (Ramón y Cajal 1909; Lorente de Nó 1937). The Golgi method stains approximately 1–5% of the cell population, revealing individual neurons or parts of neurons as opaque entities but in a mostly uncontrolled fashion (Valverde 1970). Axons and dendrites from different sources are typically intermixed and only in rare instances can a process be followed for any distance before it becomes entangled with other processes. It was within the limits of these methods that three categories of primary neurons were originally described: those neurons that innervated exclusively IHCs, those that innervated exclusively OHCs, and those that contacted both IHCs and OHCs (Retzius 1892; von Ebner 1903; Lorente de Nó 1937; Polyak, McHugh, and Judd 1946).

On the basis of somatic staining characteristics and size criteria, two populations of spiral ganglion cells have been reported (Munzer 1931;

Suzuki, Watanabe, and Osada 1963; Kellerhals, Engström, and Ades 1967; Spoendlin 1973). The problem was how to relate the two populations of ganglion cells to the three patterns of peripheral innervation. Electron microscopic observations confirmed the presence of two major populations of primary neurons: large myelinated type I ganglion cells and small unmyelinated type II ganglion cells (Spoendlin 1973). The advantage of the electron microscope is the great magnification and resolution of structural details; the disadvantage is its restricted view. Another consideration is that the tissue sections are very thin (only 70 nm thick), so for all practical purposes, it is impossible to use the electron microscope to trace processes from the cell bodies to their innervation sites in the organ of Corti. The distance involved in such a task would require thousands of sections.

Spoendlin (1973) performed some important studies that provided strong but indirect evidence for linking the two types of afferent fibers in the organ of Corti with the two types of ganglion cell bodies. He examined the nonvesiculated endings postsynaptic to the hair cells in normal cats and in cats whose auditory nerve had been severed. Nonvesiculated endings in contact with IHCs degenerated following auditory nerve damage, whereas those in contact with OHCs remained intact. By correlating the disappearance of IHC endings with the disappearance of type I ganglion cell bodies, Spoendlin postulated that type I cells must give rise to the radial fibers contacting IHCs. Since the afferent endings under OHCs and type II cell bodies remained, Spoendlin concluded that type II neurons must give rise to outer spiral fibers innervating OHCs. Spoendlin (1975) also described a so-called type III ganglion cell in his pathological cases, suggesting that they innervated OHCs, but later stated (1979) that they innervated IHCs. Type III ganglion cells are not present in normal cochleas, and their function in pathological cochleas is unknown. In the basal region of the cochleas of neonatal cats and rats, giant fibers were described in Golgi material which projected to a group of IHCs; such giant fibers, however, were not observed in animals older than a few days and their cell bodies of origin were not defined (Perkins and Morest 1975). In short, the correspondence between the separate populations of ganglion cells and the different innervation patterns in the organ of Corti depends on the age of the animal under study and the condition of its cochlea.

2.4 Current Status

Spoendlin's hypothesized innervation pattern for normal adult cats finally received direct confirmation by studies that were able to trace individual afferent fibers continuously from their cell bodies in the spiral ganglion to their terminations in the organ of Corti (Kiang et al. 1982; Ginzburg and Morest 1983; Berglund and Ryugo 1987; Brown 1987a). Cochlear

innervation in adolescent and mature animals revealed a segregated pattern of hair cell innervation. The population of large cell bodies gave rise to peripheral processes, called radial fibers, that contacted one or rarely two IHCs, whereas the population of small cell bodies gave rise to peripheral processes, called outer spiral fibers, that contacted many OHCs (Fig. 2.3).

The various descriptions in cochlear innervation may be accounted for by ignoring observations made in pathological cases and by postulating that the innervation of both IHCs and OHCs by a single fiber normally represents an immature and transient pattern. The notion that differences

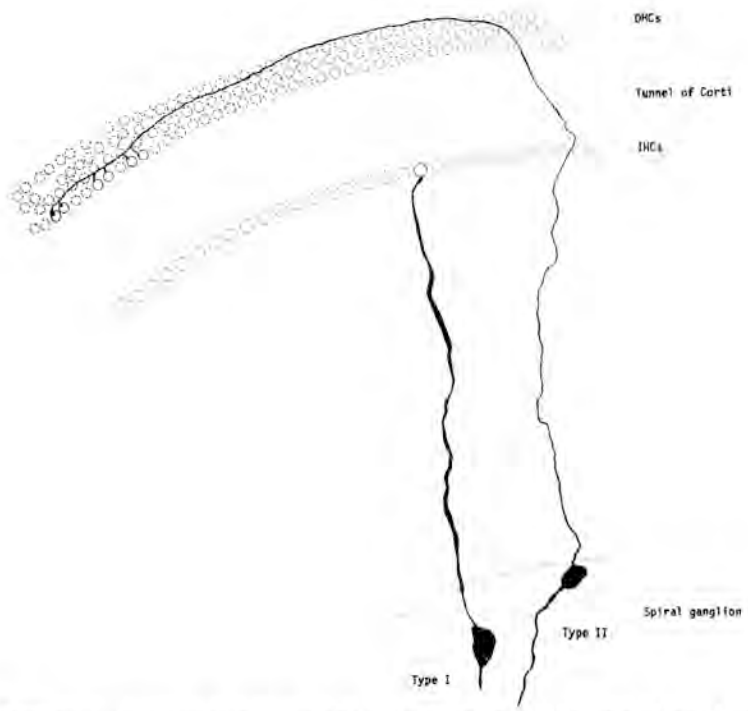

FIGURE 2.3. Composite drawing tube reconstruction of HRP-labeled type I and type II neurons in the mouse. These neurons are representative of the two populations of ganglion neurons in mammals. The type I neuron gives rise to a relatively thick process, projects radially towards the organ of Corti, and terminates on a single IHC. The type II neuron sends a continuously thin process that crosses the tunnel, spirals basally, and then terminates on several OHCs. Scale bar equals 10 μm. (From Berglund and Ryugo 1987, Wiley-Liss Publishers.)

in afferent innervation exist between cochleas of immature and mature animals is consistent with current ideas that exuberant projections retract and the innervation field becomes more restricted as the animal ages (e.g., Innocenti, Fiori, and Caminiti 1977; Jackson and Parks 1982; Stanfield and O'Leary 1985). It is now generally accepted that there is a complete segregation of pathways from the two classes of hair cell receptors by way of the two populations of primary neurons.

2.5 *Structure–Function Correlates*

The physiological responses of individual spiral ganglion neurons can be monitored as they are conveyed along the axon using microelectrodes inserted into the auditory nerve (e.g., Kiang et al. 1965; Evans 1972). All single unit activity recorded from the auditory nerve, however, is derived from the myelinated axons of type I neurons and virtually nothing is known about the response properties of type II neurons (Liberman 1982a; Robertson 1984). For these kinds of single unit recordings, it has been suggested that under a limited range of stimulus conditions the temporal pattern of discharges transmitted in any single auditory nerve fiber is qualitatively similar throughout the myelinated fiber population. Quantitatively, however, single fiber responses differ in frequency selectivity, spontaneous discharge rate, and threshold. Frequency selectivity refers to a fiber's tendency to be most sensitive to a single frequency, and is best illustrated by a "threshold tuning curve." A tuning curve describes the level and frequency coordinates of a neuron's response area to tonal sitmuli (see Fig. 3 of Evans 1972). The tip of this curve indicates the neuron's characteristic frequency (CF, that frequency to which the neuron is most sensitive) and its threshold in dB SPL to that frequency.

Since the time of von Békésy (1960), it has been accepted that the mammalian cochlea acts as a mechanical frequency analyzer, maximally sensitive to high frequencies in the basal region and sensitive to progressively lower frequencies in regions located progressively closer to the apex. Experimental verification of this notion has been derived by the mapping of frequency responses as a function of cochlear position by measuring basilar membrane motion (Rhode 1971; Khanna and Leonard 1982; Johnstone, Patuzzi, and Yates 1986), cochlear microphonic responses (Dallos 1971), IHC receptor potentials (Russell and Sellick 1978), or spike discharges recorded from the ganglion (Kohllöffel 1975; Robertson et al. 1980). Nevertheless, validation of this relationship was considered incomplete because direct access to the organ of Corti and spiral ganglion was not possible for all cochlear regions. "Place" maps were also generated by plotting the position of hair cell lesions as they related to behavioral threshold changes (Schuknecht 1953) or to alterations in the discharge patterns of auditory nerve fibers (Liberman and Kiang 1978). These latter studies suffer from some ambiguity because of the difficulty in standardizing criteria for identifying histological damage. That is, one wonders how much histological damage must be evident before function is affected, and whether hair cell appearance at the light microscopic level is sufficient criterion for accessing normal hair cell function. A definitive frequency map was finally generated for the cat by intracellular labeling of single auditory neurons of known CFs and identifying the specific IHC upon which the primary neuron terminated (Liberman 1982b). From such data we know that CF indicates the longitudinal location of the inner hair cell innervated by that fiber (Fig. 2.4). The sensitivity and range in frequency for the population of fibers reflect the hearing capabilities of the animal in question (Fay 1988).

For any particular frequency range, spontaneous discharge rate (SR) can vary from near zero to >100 spikes/sec. Spike discharges in auditory nerve fibers occur in the absence of acoustic stimulation. Fibers having different SRs display systematic differences in their threshold at CF, dynamic range, and discharge rate characteristics in response to sound (Sachs and Abbas 1974; Liberman 1978, 1990; Kim and Molnar 1979; Evans and Palmer 1980; Schalk and Sachs 1980). In the population of auditory nerve fibers, there is a striking bimodal distribution of SR where fibers tend to have rates <10 spikes/sec or >30 spikes/sec (Liberman 1978; Evans and Palmer 1980). On average, 30–40% of the fibers have SRs <20 spikes/sec and are placed in the low SR group, whereas the remaining fibers have SRs >20 spikes/sec and are placed in the high SR group. An electron microscopic study of serial sections through two IHCs at the 2.2 kHz region and two IHCs at the 2.6 kHz region revealed that each radial fiber was unbranched and formed a single synapse with one IHC (Liberman 1980a). Each IHC was innervated by 22, 26, 26, and 30 radial fibers, roughly equivalent to what has been reported for cats by

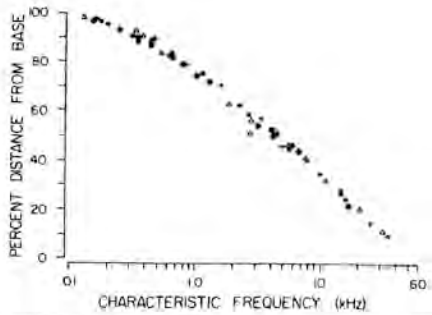

FIGURE 2.4. Relationship between CF of auditory nerve fibers and the relative location of their terminations in the cochlea. Data were determined by intracellular recording and staining methods in cats, and the different symbols are not important for our purposes. (From Liberman 1982b, AIP Publishers.)

Spoendlin (1972, 1973). Forty percent of the 104 radial fibers contacting the side of hair cell facing the modiolus were small in diameter and relatively poor in mitochondria (Liberman 1980a). In contrast, the remaining fibers were larger in diameter, richer in mitochondria, and tended to contact the side of the hair cell facing the pillar cells, but could be found anywhere along the side of the hair cell. The natural conclusion was that high SR fibers were the thicker fibers contacting the pillar side of the hair cell and that low SR fibers were the thinner fibers contacting the modiolar side of the hair cell.

A direct test of this notion was performed by labeling single auditory nerve fibers using intracellular recording and staining techniques, and these relationships were generally confirmed (Liberman 1982a). That is, high SR fibers were on average thicker in diameter and their afferent endings tended to be located on the pillar sector of the IHC. In contrast, low SR fibers were thinner and their endings were typically found in the modiolar sector of the IHC (Fig. 2.5). These differences in the anatomical and physiological properties between SR groups, present across the entire range of frequencies, suggest that the separate SR groups may play fundamentally different roles in the process of auditory perception.

3. Spiral Ganglion

In the bony core of the cochlea, a channel called Rosenthal's canal coils from base to apex in parallel with the cochlear spiral. In this channel reside the cell bodies of primary neurons, collectively called the spiral ganglion. Each cell body exhibits two processes, one extending toward the organ of Corti and the other projecting into the auditory nerve. von Ebner (1903) credits Corti as having first described the cell bodies of primary auditory neurons, circa 1850, where spiral ganglion neurons in the pig were characterized as being bipolar in shape and rather uniform in size. Only much later was the existence of at least two populations of ganglion cells reported (Munzer 1931) and subsequently confirmed on the basis of differences in size and staining properties as seen with the electron microscope (Suzuki, Watanabe, and Osada 1963; Kellerhals, Engström, and Ades 1967; Spoendlin 1973).

3.1 Cell Types

Spoendlin (1971, 1973) concluded that 90–95% of the ganglion cell population in the cat consisted of large, bipolar type I cells and 5–10% were smaller type II cells. The type I ganglion cell has a cytoplasm with a great number of ribosomes and cytoplasmic organelles, whereas the type II cell has a more filamentous cytoplasm with fewer ribosomes (Fig. 2.6). The cell bodies of type II neurons tend to lie in the periphery of Rosenthal's

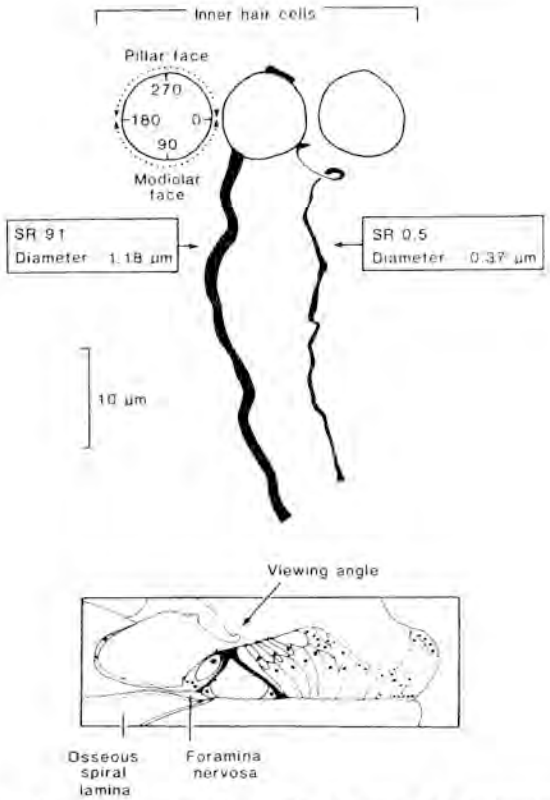

FIGURE 2.5. Schematic drawing of two radial fibers and their terminations upon a single IHC when viewed from above. OHCs would be toward the top of the figure. The high SR fiber is thicker and terminates on the pillar side of the IHC. In contrast, the low SR fiber is thinner and terminates on the modiolar side of the IHC. (From Liberman 1982a, AAAS Publishers.)

canal, towards the osseous spiral lamina (Robertson 1984; Berglund and Ryugo 1987). The histological affinity of type II cell bodies for neurofilament stains (Kiang et al. 1984; Berglund and Ryugo 1986) is consistent with the specific labelling by protargol of proteins that form neurofilaments (Gambetti, Antilio-Gambetti, and Papasozomenos 1982).

Monoclonal antibodies directed against the 200 kD neurofilament protein have unambiguously labeled the cell bodies of type II neurons of the mammalian spiral ganglion (Berglund and Ryugo 1986, 1991; Romand, Hafidi, and Despres 1987). Because tissue stained with basic dyes or protargol still has the cell types intermixed, one principal advantage of

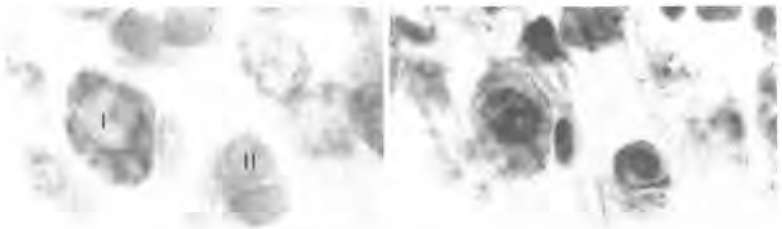

FIGURE 2.6. Left panel: Toluidine blue staining of cochlear spiral ganglion neurons in rat. The type II neuron (II) is distinguished by its small cell body, pale cytoplasm, and dark staining nucleus. The type I neuron (I) has a larger cell body, displays prominent Nissl bodies in its cytoplasm, and has a pale staining nucleus. A satellite cell nucleus is evident against the bottom of the type II neuron and against the side of the type I neuron. Right Panel: The same cells as shown on the left but stained with protargol (and at a slightly different focal plane). The type II cytoplasm and nucleus are darkly stained. In contrast, the nucleus but not the cytoplasm of the type I stains darkly. The implication is that the cytoplasm of type I neurons is rich in ribosomes, whereas that of type II neurons is rich in neurofilaments. Scale bar equals 10 μm. (From Berglund and Ryugo 1986, Elsevier Publishers.)

immunostaining is that positively labeled structures are obviously distinct from unlabeled structures (Fig. 2.7). Furthermore, it was shown that the epitope in type II neurons is phosphorylated because removal of phosphate groups resulted in no staining of ganglion cell bodies, and immunostaining cochlear tissue with antibodies directed against the nonphosphorylated 200 kD neurofilament protein labeled both types of ganglion cells. Monoclonal antibodies directed against the 68 kD or 160 kD neurofilament proteins also labeled the somata of both types of ganglion cells. The antibody method is consistent with ultrastructural descriptions of neurofilament distribution and is able to label selectively the population of type II neurons in a variety of mammals including humans (Berglund and Ryugo 1991). Under normal circumstances, this method can greatly facilitate studies involving counts of type II neurons, plots of their distribution within the ganglion, or morphometry. The application of immunocytochemical techniques may also prove useful for grouping ganglion cell subpopulations by identifying molecules associated with particular structural proteins, metabolic enzymes, or neurotransmitter candidates.

The most unambiguous distinction between the two types of ganglion cells is their segregated innervation of inner versus outer hair cells. Other somatic characteristics of ganglion cells are not universal across species. For example, the presence of a myelin sheath around type I neurons is

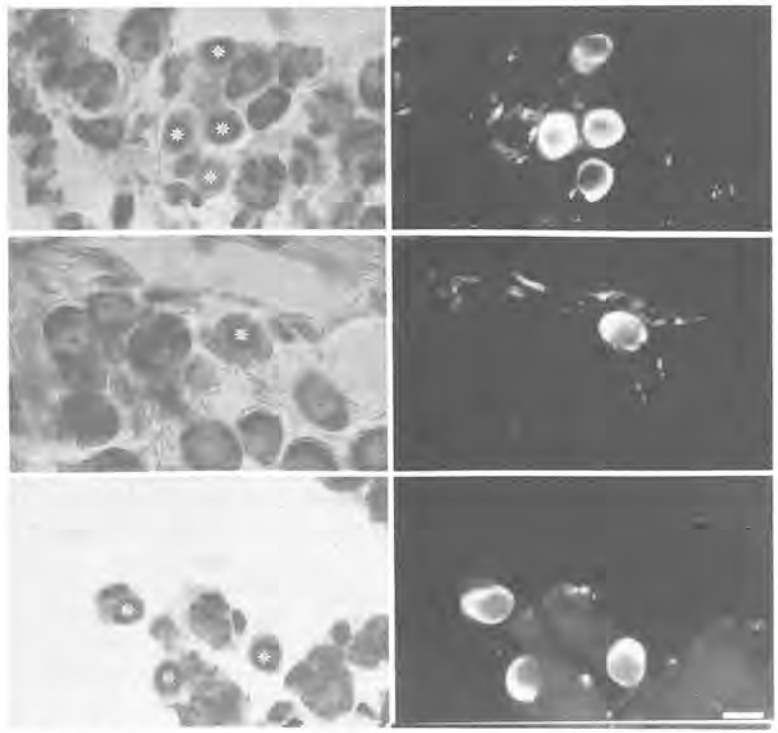

FIGURE 2.7. Immunostaining of type II neurons in rat spiral ganglion. The left panel shows tissue stained with toluidine blue and the right panel shows the same tissue stained with the antibody RT-97. Note how the type II neurons (stars) are preferentially labeled with this antibody which is directed against the phosphorylated 200-kD neurofilament protein. (From Berglund and Ryugo 1986, Elsevier Publishers.)

frequent but not constant; there are as many myelinated as unmyelinated small cells in the human (Ota and Kimura 1980). In the cat, the nucleus of type II neurons is eccentric and lobulated, but such is not the case in humans and rodents (Spoendlin 1981, 1982; Spoendlin and Schrott 1988). Somatic shape is also distinctive in cats where type I neurons tend to be bipolar and type II neurons tend to be pseudomonopolar (Kiang et al. 1982), but in rodents, nearly all ganglion cells appear bipolar (Berglund and Ryugo 1987, 1991; Brown et al. 1988a). Structural idiosyncracies have been found in the cochleas of the macaque monkey where two new ganglion cell classes have been described in addition to the usual type I and type II categories. Dendrodendritic synapses were observed within

Rosenthal's canal, presumably between the peripheral processes of type II ganglion cells, and synapses of efferent and sympathetic origin were found on the perikarya and processes of the unmyelinated neurons (Kimura 1986, 1987). Finally, the distinctions in cell body size between the two cell types diminish as the size of the animal decreases (Brown et al. 1988a). Clearly, more studies of a comparative nature are required in order to fully appreciate the functional significance of these variations.

3.2 Process Characteristics

In the vicinity of the cell body, the processes of the two types of ganglion cells differ in appearance (Kiang et al. 1982; Berglund and Ryugo 1987; Brown 1987a; Brown et al. 1988a). In the cat, for example, the larger type I neurons exhibit a peripheral process whose average diameter is much smaller (0.56 μm) than that of the central process (1.73 μm). In contrast, the type II neurons exhibit processes whose mean diameters are virtually identical (central = 1.25 μm; peripheral = 1.23 μm; Kiang et al. 1982). For the smaller rodents (mice and gerbils), the processes of type II neurons must extend some 100–200 μm away from the cell body before unambiguous diameters differences can be discerned (Berglund and Ryugo 1987; Brown et al. 1988a) In rodents, type II processes gradually taper to less than 1 μm in diameter, whereas type I processes remain relatively constant at 1–2.5 μm in diameter). As the body weight of the species decreases, so does the distinction between the two populations of ganglion cells using cell body silhouette area (Fig. 2.8). Irrespective of these morphologic variations, it is accepted that there are two principal ganglion cell classes.

Type I neurons appear to have a spatial organization within the ganglion. The cell body silhouette area is largest (on average 350 μm^2) for low frequency neurons (<0.2 kHz) and becomes progressively smaller until it levels off (275 μm^2) at about 4 kHz; cell body area does not appear to be related to SR (Liberman and Oliver 1984). The position of intracellularly labeled ganglion cell bodies was mapped along the length of Rosenthal's canal as a function of CF in cats (Keithley and Schreiber 1987). The frequency of organization of the ganglion is similar to that of the organ of Corti: low frequencies are located apically and progressively higher frequencies are located at progressively more basal regions. There is also a spatial relationship between SR and cell body location within Rosenthal's canal (Kawase and Liberman 1991). That is, auditory nerve fibers tend to maintain the regional segregation established at the IHC in the spiral ganglion. Fibers of low SR are much more common in the half of the ganglion nearest scala vestibuli, whereas fibers of high SR fibers are more common in the region of the ganglion nearest scala tympani. This observation is consistent with fibers leaving the organ of Corti and not crossing each other. The modiolar side of the IHC projects

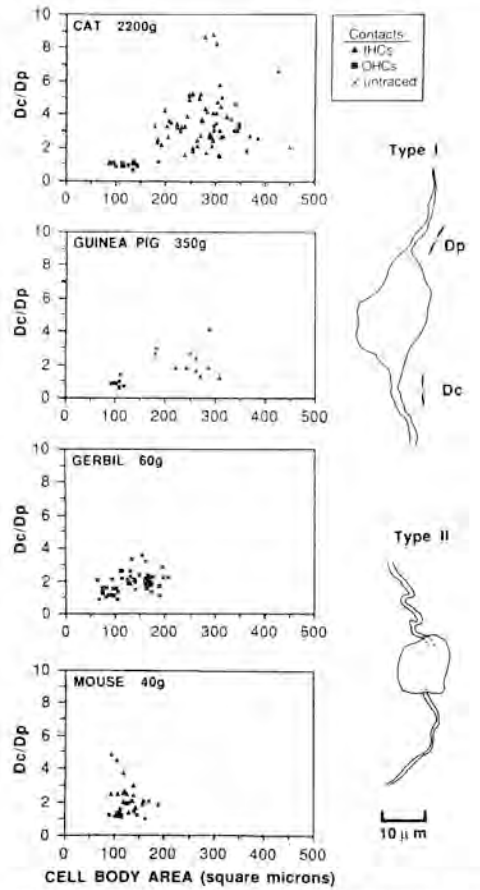

FIGURE 2.8. Morphometry of HRP-labeled spiral ganglion neurons from four species. The legend indicates those neurons whose processes were traced to IHCs, OHCs, or could not be traced to their endings. The ratios of the diameters of the central (Dc) and peripheral (Dp) processes are plotted against cell body silhouette area. Right: drawing tube reconstructions of labeled ganglion cells showing the segments over which Dc and Dp were measured. The drawings are from a type I neuron traced to an IHC and a type II neuron traced to OHCs in a guinea pig. (From Brown et al. 1988a, Wiley-Liss Publishers.)

through the scala vestibuli pole of the ganglion and the pillar side of the IHC projects through the scala tympani pole of the ganglion. These data directly confirm a previously proposed feature of spatial organization within the ganglion (Leake and Snyder 1989).

4. Central Projections

4.1 Auditory Nerve

Fibers of the auditory nerve travel in the central core of the cochlea, called the modiolus, toward the cochlear nucleus in the brain. There are approximately 50,000 fibers in cat, 31,400 fibers in human, 31,250 fibers in rhesus monkey, 31,240 fibers in squirrel monkey, 24,000 fibers in guinea pig, 15,800 in rat, and 12,250 in mouse (Rasmussen 1946; Gacek and Rasmussen 1961; Alving and Cowan 1971; Ehret 1979; Keithley and Feldman 1979). Irrespective of absolute fiber counts, the nerve contains roughly 90–95% thick, myelinated fibers and 5–10% unmyelinated fibers (Alving and Cowan 1971; Arnesen and Osen 1978; Anniko and Arnesen 1988). Recent evidence in cats unambiguously demonstrated that thick fibers are myelinated and arise from type I cell bodies and that thin fibers are unmyelinated and arise from type II cell bodies (Fig. 2.9; Ryugo et al. 1991). The proportion of myelinated and unmyelinated fibers matches the proportion of the two types of ganglion cell bodies for other mammals (Kiang et al. 1984), thereby making the argument extremely strong that

FIGURE 2.9. Electronmicrograph of an HPR-labeled thick and thin fiber in the auditory nerve. The thick fiber is myelinated and arises from a type I spiral ganglion neuron. The thin fiber (arrow) is unmyelinated and arises from a type II spiral ganglion neuron. Scale bar equals 0.5 μm. (From Ryugo et al. 1991, Wiley-Liss Publishers.)

the two types of fibers in the auditory nerve arise respectively from the two types of ganglion cells.

The diameters of the myelinated fibers appear, on average, to be thicker for apical fibers and thinner for basal fibers in cat, squirrel monkey, and mouse (Alving and Cowan 1971; Arnesen and Osen 1978; Liberman and Oliver 1984; Anniko and Arnesen 1988). The diameter difference across these particular species is roughly 0.5 μm. For all frequencies, the axons of high SR fibers are thicker on average than those of low SR fibers (Liberman and Oliver 1984; Kawase and Liberman 1991). It also appears that axons get progressively thicker with increased distance from the cell body. At 1–2 mm from the ganglion, diameters tend to stabilize following as much as a 50% increase.

Fibers originating from the apex of the cochlea occupy the middle of the nerve trunk with more basal fibers spiralling and coursing peripheral to the more apical ones (Arnesen and Osen 1978). This spatial arrangement of cochlear fibers is orderly within the nerve trunk and continues into the cochlear nucleus (Sando 1965; Arnesen, Osen, and Mugnaini 1978), and is reflected by the tonotopic organization of the nerve (Liberman and Kiang 1978). It seems that both fiber types adhere to this cochleotopic relationship (Brown et al. 1988a).

4.2 Cochlear Nucleus

4.2.1 Type I Fibers

The myelinated auditory nerve fibers are qualitatively similar to one another. Figure 2.10 illustrates several features common to most fibers. The "root branch" crosses the Schwann-glia border, ascends for a distance into the nucleus, and then bifurcates. This characteristic bifurcation gives rise to an ascending branch and a descending branch. The ascending branch is directed anteriorly through the anteroventral cochlear nucleus (AVCN) and the descending branch is directed posteriorly through the posteroventral cochlear nucleus (PVCN), toward and usually into the dorsal cochlear nucleus (DCN). The ascending, descending, and root branches generally maintain straight trajectories, exhibit the largest diameters, and are commonly referred to as "parent" branches.

4.2.2 Root Branch

The portion of the fiber extending between the spiral ganglion and the bifurcation was classically called the radicular or root branch (Ramón y Cajal 1909). The total length of this root branch, whether originating from apical or basal regions, is approximately the same, namely 7 to 8 mm from their entrance into the spiral lamina to the tips of their ascending branches (Arnesen and Osen 1978; Fekete et al. 1984). Although the cell bodies of basal fibers are "closer" to the Schwann-glia border

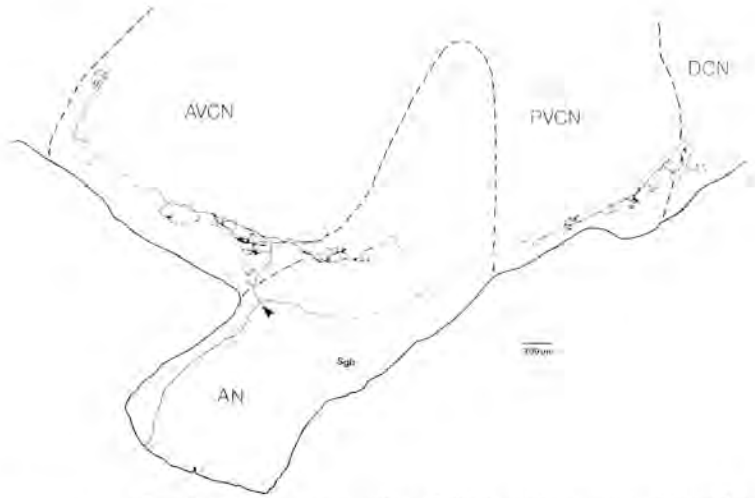

FIGURE 2.10. Drawing tube reconstruction of single auditory nerve fiber (CF = 0.45 kHz, SR = 1.2s/s) in a left cochlear nucleus. Anterior is toward the left and dorsomedial is toward the top. Upon entering the nucleus, the root branch bifurcates (arrowhead) to form the ascending and descending branches. This fiber forms a relatively planar arborization within the nucleus whose spatial position is related to the location of the bifurcation. Abbreviations: AN, auditory nerve; AVCN, anteroventral cochlear nucleus; DCN, dorsal cochlear nucleus; PVCN, posteroventral cochlear nucleus; Sgb, Schwann-glial border. (From Ryugo and Rouiller 1988, Wiley-Liss Publishers.)

than are those of apical fibers, the axons of basal fibers must penetrate further into the nucleus before bifurcating and arborizing. That is, fibers arising from the apex (the low-frequency region) ramify just after crossing the Schwann-glia border to distribute endings in the ventral portion of the cochlear nucleus. Fibers arising from progressively more basal regions of the cochlea (higher-frequency regions) bifurcate and arborize in progressively more dorsal regions of the cochlear nucleus (Fig. 2.11). This orderly arrangement in the distribution of auditory nerve fibers represents what is termed a "cochleotopic" projection, observed originally in Golgi stained material (Ramón y Cajal 1909; Lorente de Nó 1933).

This cochleotopic projection has been verified by several different methods. One method was a population approach where small lesions were placed in different locations along the cochlear spiral, and the resulting distribution of silver grains attracted by degenerating fibers and terminals was plotted (Sando 1965; Osen 1970; Webster 1971; Moskowitz and Liu 1972; Noda and Pirsig 1974). Other population studies made

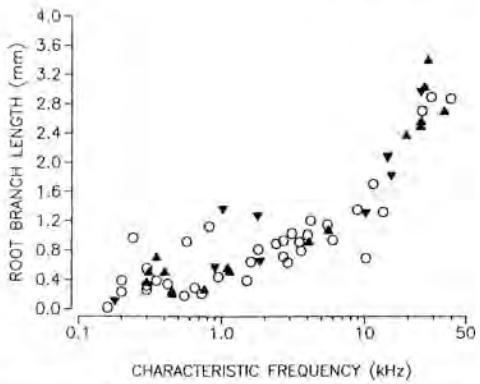

FIGURE 2.11. Relationship of fiber CF to root branch length (measured from Schwann-glia border to bifurcation). These data reveal that the location of the bifurcation is systematically related to fiber CF ($r = 0.95$, $p < 0.001$) but not fiber SR. Symbols: Open circles, SR > 18 s/s; filled triangles, SR < 18 s/s.

small HRP deposits in restricted sectors of the spiral ganglion and mapped the distribution of anterogradely labeled central axons (Leake and Snyder 1989; Brown and Ledwith 1990). From both types of anterograde tracing studies, projection "bands" of stained fibers and terminals were revealed whose regional locations corresponded systematically to the lesion or injection site in the cochlea. The other method used the intracellular technique where the task was to record the characteristic frequency of a single fiber, inject the fiber with HRP, and then reconstruct the labeled axonal arborization within the cochlear nucleus (Fig. 2.12). These results of auditory nerve projections (Fekete et al. 1984; Rouiller and Ryugo 1988; Ryugo and Rouiller 1988; Wright et al. 1991) are consistent with the electrophysiological data reporting the tonotopic organization for the cochlear nucleus (Rose, Galambos, and Hughes 1959; Bourk, Mielcarz, and Norris 1981; Spirou, May, and Ryugo 1989).

4.2.3 Ascending Branch

For every auditory nerve fiber, the ascending branch arises at the bifurcation of the root branch, exhibits a relatively straight trajectory into the anterior division of the AVCN, and terminates as a large, axosomatic ending called the endbulb of Held (Ramón y Cajal 1909). The mean ($\pm$ SD) length of the ascending branch is relatively uniform (2.33 $\pm$ 0.53 mm in cat) and unrelated to fiber CF or SR. Each parent branch gives rise to an average of nine primary collaterals, a number also unrelated to fiber CF or SR (Fekete et al. 1984). The collateral ramifications of most ascending branches, especially those of high SR fibers, are short and

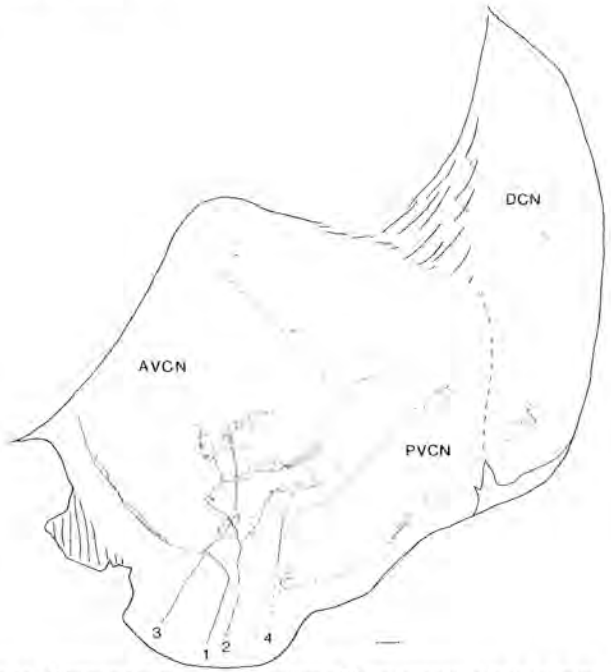

FIGURE 2.12. Drawing tube reconstruction of four intracellularly labeled auditory nerve fibers in a left cochlear nucleus. There is a systematic relationship between fiber CF and location of arborization in the nucleus, but its manifestation can be distorted when viewed in only two dimensions. In the AVCN, for example, the ascending branches of fiber 2 and fiber 3 project out of the plane of the paper towards the viewer. Fiber 1 has no descending branch, CF = 0.2 kHz, SR = 112 s/s; Fiber 2, CF = 1.2 kHz, SR = 1.1 s/s; Fiber 3 has a descending branch that does not enter the DCN, CF = 4.5 kHz, SR = 49.6 s/s; Fiber 4, CF = 20 kHz, SR = 61 s/s. AVCN, anteroventral cochlear nucleus; PVCN, posteroventral cochlear nucleus; DCN, dorsal cochlear nucleus. (Scale bar equal 100 μm.)

relatively simple. The relative thickness of terminal collaterals roughly corresponds to the size of the terminal swellings. The overall complexity of the ascending branch arborization, however, is strongly correlated to fiber SR (Fekete et al. 1984; Ryugo and Rouiller 1988). In cat, the number of branch points for low SR fibers is on average, more than twice than that for high SR fibers. The number of branch points plus one equals the number of terminal swellings, and the number of terminal swellings is a rough estimate of the number of neurons synaptically contacted by that fiber. In addition, the mean collateral length for low SR fibers is 55% greater than that of high SR fibers, indicating that synaptic information for low SR fibers is distributed to a wider region.

One interpretation for these observations is that low SR fibers convey information to more neurons distributed over a wider region of the AVCN than do high SR fibers. The data may be related to an idea proposed by Stevens and Davis (1938) in which the perception of loudness was hypothesized to be proportional to the number of active neurons. The excitation of high threshold, low SR fibers by loud sounds would not only increase the pool of active auditory nerve fibers but also could produce a spread of activity to many additional neurons in the AVCN. Such recruitment might be important because a saturation of discharge rate for high SR fibers is already produced by only moderate levels of sound.

There is also circumstantial evidence implicating low SR fibers as part of the neural circuit mediating the middle ear muscle reflex. This reflex occurs in the presence of a loud noise whereby muscles of the middle ear contract and exert feedback control on the cochlear response (Borg 1972). The sensory limb of this reflex passes through the auditory nerve, and the unmyelinated fibers can be eliminated from consideration because their conduction time will be too long (>10 msec) to permit their participation in the reflex (Kiang, Keithley, and Liberman 1983). Neurons that reside in the AVCN apparently contribute to this reflex because transection of the output pathway of the AVCN abolishes the reflex; there is no change in the reflex following transection of the output pathways of the DCN or the PVCN (Borg 1973). The low SR fibers have high thresholds, and therefore are still within their operating range in the presence of loud sounds (85–95 dB) that evoke the middle ear muscle reflex (Liberman and Kiang 1984). Since it is in the AVCN where low SR fibers exhibit their arbor specializations, the current task is to discover which neurons might preferentially receive inputs from the low SR fibers and project in turn to the motor nuclei of cranial nerves V and VII.

4.2.4 Descending Branch

The descending branch is directed posteriorly through the PVCN and usually (85% of the cases), but not always, enters the DCN (Fekete et al. 1984). In cats, each parent branch is 3.38 ± 0.64 mm in length and gives rise to an average of 11 primary collaterals. The morphology of the descending branch arborization appears to be independent of fiber SR, but there are some features of the fiber that are related to fiber CF. Auditory nerve fibers having CFs below 1–2 kHz do not enter the central region of the PVCN, known as the octopus cell region; not surprisingly, low-frequency units are poorly represented in this region (Ritz and Brownell 1982).

On the other hand, fibers with CFs greater than 4 kHz emit collaterals which stream ventrally in long parallel arrays (Fig. 2.12). The orientation of this streaming is perpendicular to the descending parent but roughly parallel to the primary dendrites of octopus cells. Octopus cells represent

a physiological class of "on" units, which respond primarily at the onset of a tone burst (Godfrey et al. 1975; Ritz and Brownell 1982). This assignment has been directly confirmed in which "on" units were intracellularly labeled with HRP (Rhode et al. 1983; Rouiller and Ryugo 1984). In general, "on" units are among the most broadly tuned cells in the PVCN when measured 20 dB above threshold, yet when measured at 10 dB above threshold they are as sharply tuned as other unit types in the PVCN (Godfrey et al. 1975). The parallel alignment of dendrites and collateral ramifications may provide an anatomical basis for both the sharpness of frequency selectivity near threshold and the broad tuning at higher intensities. Certain spatial relationships might permit a maximal number of synaptic contacts to be made between a few fibers of similar CFs and the dendrites of a particular octopus cell. Such input would be expected to dominate the cell's response at low stimulus levels, thereby accounting for the sharp tuning near threshold. Primary fibers having higher or lower CFs would make relatively fewer contacts with that octopus cell because of spatial restrictions; consequently, at low stimulus levels, their inputs would not be sufficient to activate the cell. At higher stimulus levels, more primary fibers representing a wider range of frequencies would be activated and their summed activity converging onto the octopus cell might account for the broader frequency response (compared to other cochlear nucleus units or auditory nerve fibers).

Upon entering the DCN, individual fibers ramify and terminate within a relatively narrow band of the deep polymorphic layer, also called layer III (Fig. 2.12). Rarely do fibers reach as far as the fusiform or pyramidal cell layer (also called layer II); no terminals were ever observed in the molecular layer although fibers occasionally passed through this layer on their way elsewhere. The arborization in DCN is sparse, producing only a few *en passant* and terminal swellings. These swellings are relatively small and are found in the neuropil. The topographic banding of terminal arbors in the DCN (Wright et al. 1991) is consistent with the tonotopic arrangement of this nucleus (Rose, Galambos, and Hughes 1959; Spirou, May, and Ryugo 1989).

4.2.5 Type II Axons

There is evidence that the unmyelinated fibers maintain a cochleotopic projection into the nucleus. When the central axons of type II spiral ganglion neurons are traced into the cochlear nucleus, their bifurcations are typically clustered tightly around the bifurcations of the myelinated axons. Likewise, most type II axons send branches toward the AVCN and PVCN following the labeled type I axons from the same region of the spiral ganglion (Brown 1987a; Brown et al. 1988a). Individual type II axons were completely reconstructed along with those of type I axons in gerbil and mouse from basal regions of the cochlea, and both fiber types

were overlapping in their trajectories (Fig. 2.13). In the mouse, type II fibers from various cochlear regions exhibit a cochleotopic projection (Berglund and Brown 1989).

Type II axons differ markedly from type I fibers in the complexity of their arborizations (Brown et al. 1988a; Ryugo et al. 1991). In gerbil, type I fibers give rise to an average ($\pm$ SD) of 29 $\pm$ 9 primary collaterals and 80 $\pm$ 27 terminal swellings. In contrast, type II fibers exhibit 4 $\pm$ 2 pri-

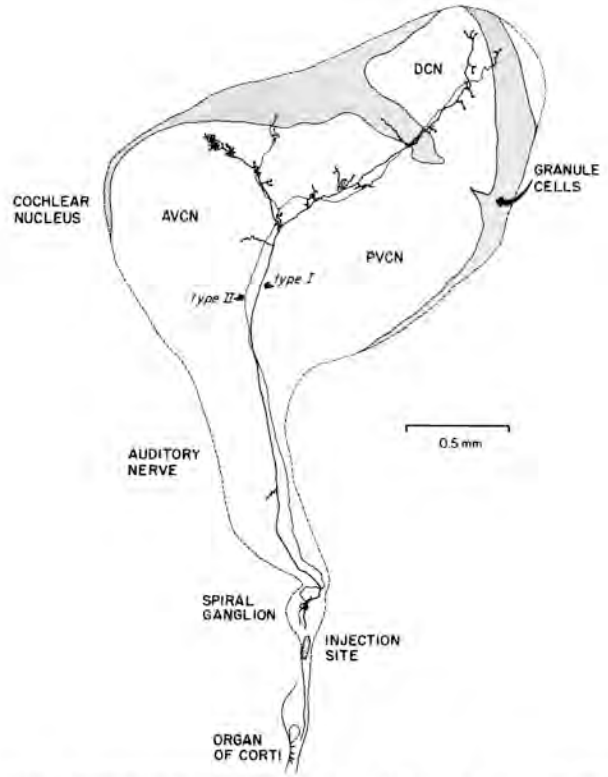

FIGURE 2.13. Drawing tube reconstruction of the central axons of an identified type I neuron (thick line) and an identified II neuron (thin line) through the auditory nerve and into the cochlear nucleus of a gerbil. Although the trajectories of these fibers are similar, the terminations of type II neurons are consistently separated from those of type I neurons because they project into granule cell regions. This drawing is a two-dimensional projection of 21 sections, each 80 μm in thickness. AVCN, anteroventral cochlear nucleus; PVCN, posteroventral cochlear nucleus; DCN, dorsal cohlear nucleus. (Modified from Brown et al. 1988a, Wiley-Liss Publishers.)

mary collaterals and 7 ± 3 terminal swellings; these terminal swellings are all bouton endings. Although the axon trajectories coincide with those of type I fibers, their final destination is in regions containing high densities of granule cells. That is, the terminal swellings of type II projections are distributed in granule cell regions of the dorsal and lateral VCN, the granule cell lamina separating the DCN from the VCN, and the granule cell layer of the DCN. Furthermore, there is a general size difference between the terminal swellings of the two fiber types (Fig. 2.14). For completely reconstructed type II fibers, there was an average of 128 ± 62 *en passant* swellings central to the cell body (Brown et al. 1988a). Many *en passant* swellings examined with the electron microscope, however, did not form synapses and instead, appeared as empty varicosities typical of a pathological condition (Ryugo et al. 1991). Because it is not known to what extent *en passant* swellings are synaptic, it is unknown whether type I and type II fibers share the same synaptic targets. If, however, *en passant* swellings tend not to be synaptic, then the two types of fibers may have completely segregated synaptic connections with neurons in the cochlear nucleus. This issue is important because ideas regarding how

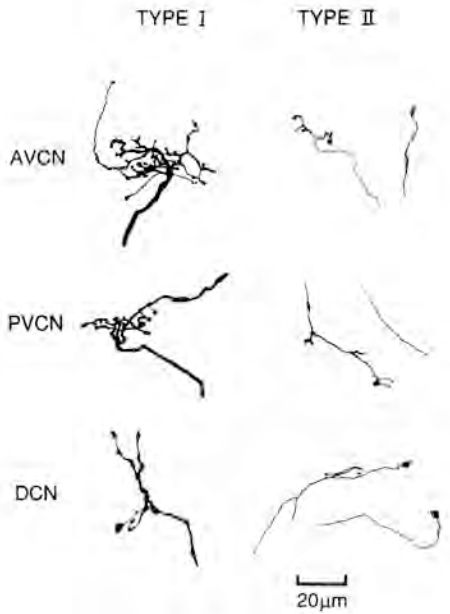

FIGURE 2.14. Drawing tube tracings of terminal swellings typical for type I and type II neurons in the mouse. Type II neurons exhibit thinner fibers and generally smaller terminals than do type I neurons. (From Brown et al. 1988a, Wiley-Liss Publishers.)

the central nervous system processes information from the hair cell receptors will depend substantially on whether the two primary fiber types have separate or overlapping connections.

4.2.6 Type I Fiber Ending Categories

Terminal boutons are the most common category of ending and the endbulbs of Held are the most conspicuous for type I auditory nerve fibers (Fig. 2.15). Held (1893) originally suggested on the basis of analysis of Golgi material in kittens that boutons and endbulbs were the two types of endings emitted by auditory nerve fibers. This conclusion has generally been supported by subsequent investigations in other animals (Ramón y Cajal 1909; Lorente de Nó 1933; Harrison and Irving 1966; Feldman and Harrison 1969; Brawer and Morest 1975). In the mature cat, the majority of endings fall into one of the these two groups although some endings, called modified or small endbulbs, have distinctly intermediate characteristics (Rouiller et al. 1986).

All ending types were found on the ascending branch and all but endbulbs were found on the descending branch. As a result, there is a considerable range in ending size within the VCN. In contrast, the DCN contains a fairly homogeneous population of small primary endings. Despite the variations in morphological appearance, HRP-labeled endings in adult cats could be placed into one of three descriptive categories on the basis of size and shape. Each category showed specific characteristics with respect to spatial distribution in the cochlear nucleus, yet the proportion of the different ending categories appears independent of the fiber CF or SR.

Small endings (approximately 5–7 μm^2) were primarily terminal boutons, represented 94% of all endings, and were distributed throughout the neuropil of the cochlear nucleus. Terminal boutons of low SR fibers are on average 1.5 μm^2 smaller but more numerous compared to those of high SR fibers, a difference especially pronounced for the ascending branch ($p < 0.01$). There is no light microscopic appearance of a relationship between bouton morphology and fiber CF. *En passant* swellings are small (approximately 4 μm^2), constant in size for both SR groups of fibers, and distributed in neuropil. Because they were not always found to form synapses, they are not strictly considered endings (Rouiller et al. 1986).

Intermediate endings (20–40 μm^2) consisted of modified endbulbs which mostly formed axosomatic contacts. This category composed 4% of the ending population and was found in close proximity to the perikarya of primarily globular cells, but also of octopus and spherical cells. These endings from low SR fibers were on average smaller than those of high SR fibers, but there was no difference in numbers. Furthermore, these endings did not vary in their parent branch distribution with respect

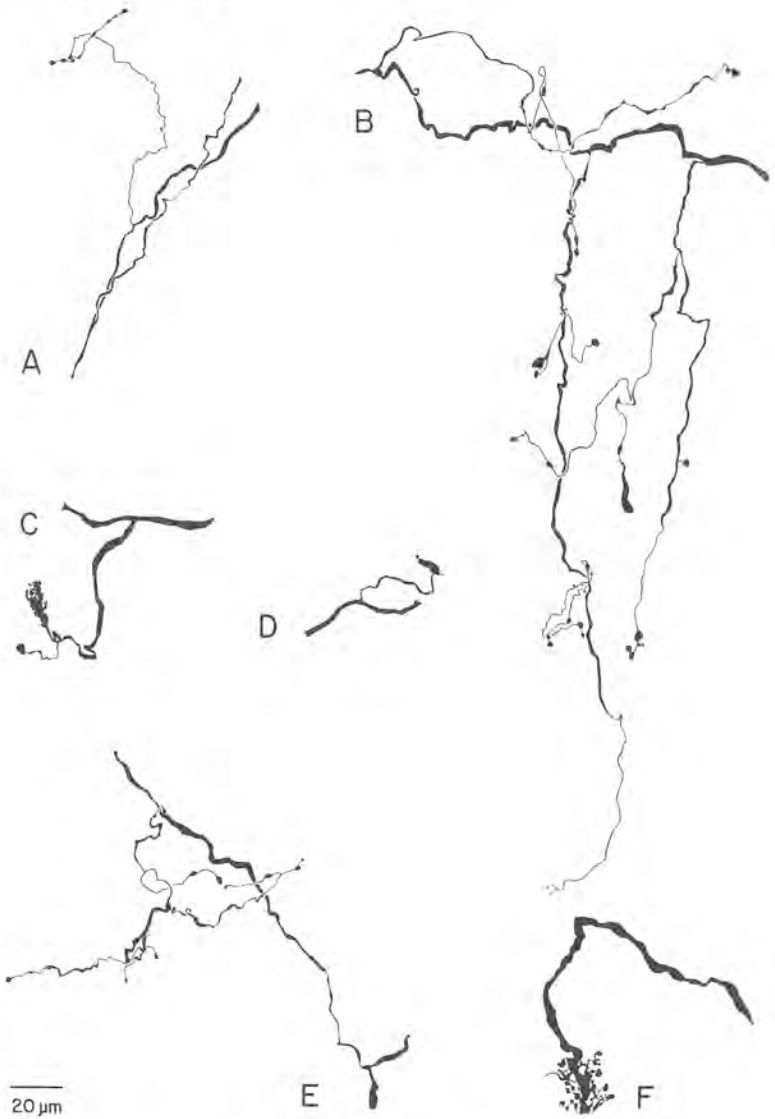

FIGURE 2.15. Selected collaterals and endings of a type I fiber. (A) Terminal boutons and *en passant* swellings in the deep layer of the DCN; (B) Long, ventrally directed collaterals terminate as boutons of varying size in the central region of the PVCN; (C, D) Small "modified" endbulbs terminating against the cell bodies of globular cells in the region of the auditory nerve root; (E) Terminal boutons and *en passant* swellings in the AVCN; (F) Endbulb of Held in the anterior division of the AVCN. (From Fekete et al. 1984, Wiley-Liss Publishers.)

to fiber SR, nor did they exhibit morphological features related to fiber CF.

The third category of endings contained exclusively endbulbs of Held (Fig. 2.16). These large endings (200–350 μm^2) represent 2% of the ending population and make axosomatic contact with spherical cells in the anterior division of AVCN and occasionally with globular cells in the posterior division of AVCN. Fibers having CFs below 4 kHz gave rise to the largest endbulbs. There were no systematic variation in endbulb size or branch distribution that correlated with fiber SR.

The similarity in average endbulb size across the SR groups was unexpected, especially in light of their differences in appearance. That is, endbulbs of high SR fibers tend to have larger but fewer swellings and lobules compared to endbulbs of low SR fibers (Fig. 2.17). There is a subjective impression that low SR fibers gave rise to lacy, delicate structures, yielding endbulbs that appear to have greater complexity in form. The ratio, silhouette area divided by silhouette perimeter (with the units dropped), was used to provide an objective value for representing each endbulb. This value is referred to as a "form factor" and it separated endbulbs into two almost nonoverlapping populations according to fiber SR, irrespective of fiber CF or endbulb size (Sento and Ryugo, 1989). Endbulbs from low SR fibers had form factors <0.52, whereas those from high SR fibers had form factors >0.52. These endbulb observations, coupled with root branch length data (Fig. 2.11), suggest that two fundamental properties of auditory nerve fibers, CF and SR group, can be

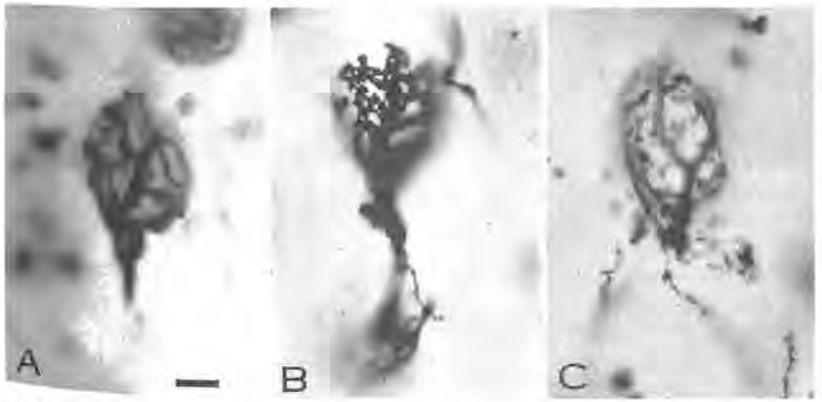

FIGURE 2.16. Photomicrographs of endbulbs of Held in the anterior division of the AVCN from adult cats. Endbulb morphology is revealed by (A) HRP methods, (B) Golgi-Kopsch methods, and (C) Golgi-Cox methods. Scale bar equals 10 μm. (From Ryugo and Fekete 1982, Wiley-Liss Publishers.)

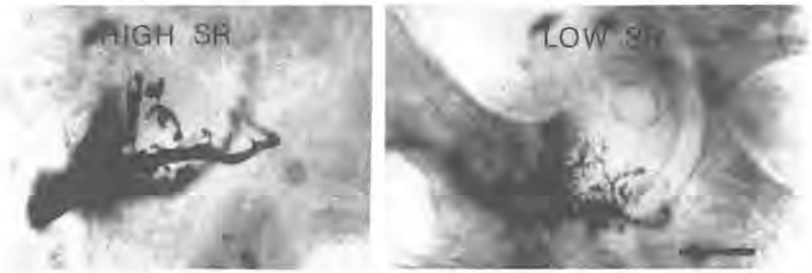

FIGURE 2.17. Photomicrographs of endbulbs revealing SR-related differences in morphology. The endbulb from a high SR fiber (CF = 1.1 kHz, SR = 56 s/s) is compared to that from a low SR fiber (CF = 1.0 kHz; SR = 0.01 s/s). These endbulbs are from the same cat but opposite cochlear nuclei. Note that the endbulb from the low SR fiber has more but smaller lobulations and swellings compared to that of the endbulb from the high SR fiber. Scale bar equals 10 μm. (From Ryugo and Sento 1991, Wiley-Liss Publishers.)

roughly estimated without having to perform the difficult intracellular electrophysiological experiments.

4.2.7 Primary Synapses

Electron microscopic studies have revealed at least four types of terminals that may be distinguished on the basis of differences in synaptic vesicle size and shape, all of which make synaptic contact with second order neurons of the cochlear nucleus (Lenn and Reese 1966; Cohen 1972; Gentschev and Sotelo 1973; Ibata and Pappas 1976; Cant and Morest 1979; Tolbert and Morest 1982). For the purpose of this review, it is significant that all terminals having large (approximately 50–60 nm in diameter), clear, round vesicles disappear after cochlear ablation (Cohen 1972; Cant and Morest 1979; Tolbert and Morest 1982). Such terminals have the same morphological features as those labeled with HRP following extracellular deposits in the auditory nerve (Ryugo and Fekete 1982) or intracellular injections of individual type I auditory nerve fibers (Rouiller et al. 1986; Ryugo and Sento 1991). In typical HRP-labeled endings, mitochondria, numerous clear, round vesicles, and postsynaptic densities are visible (Fig. 2.18). The vesicles, 54.5 $\pm$ 4.4 μm (mean $\pm$ SD) in diameter, accumulate on the presynaptic side of the synapse, in close proximity to a thickening of the cell membrane. The extracellular space in this region is slightly widened and contains a thin band of dense, fuzzy material. A segment of the postsynaptic cell membrane exhibits a prominent density that is coextensive with the thickened presynaptic membrane, giving the synaptic contact an asymmetrical appearance. The

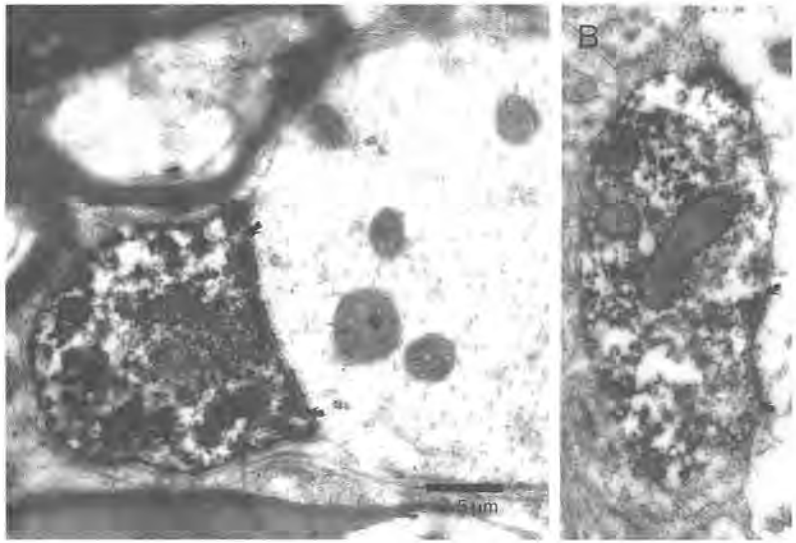

FIGURE 2.18. Electron micrographs comparing the morphology of the central synapses from terminals of type II (A) and type I (B) spiral ganglion neurons in cat. The terminal of the type II neuron contains small round vesicles and a membrane apposition that is largely synaptic (flanked by arrows). In contrast, the terminal of the type I neuron contains large round vesicles and a punctate postsynaptic density (arrows). (From Ryugo et al. 1991, Wiley-Liss Publishers.)

synapse is relatively small (Fig. 2.18, arrows) compared to the total membrane apposition. In the case of the endbulbs, the postsynaptic density often exhibits a slight convexity, whereas for boutons, the postsynaptic density is typically flat. Twenty HRP-labeled terminals in different regions of the cochlear nucleus from intracellularly characterized type I auditory nerve fibers have been examined, and qualitatively, they all have similar morphology (Rouiller et al. 1986).

Synapses from type I auditory nerve fibers are distributed throughout the cochlear nucleus, primarily against cell bodies and dendrites. These terminations do not enter the superficial granule cell regions of the dorsal and lateral parts of the VCN, the lamina of granule cells separating the DCN from the VCN, or the granule cell and molecular layers of the DCN (Osen 1970; Fekete et al. 1984; Brown et al. 1988a). The implication is that type I primary fibers connect with neurons which project axons to higher auditory centers. This situation is in marked contrast to that of type II fibers, which most likely connect with local circuit neurons of the granule cell regions (Fig. 2.18A). The synaptic region of type II fibers is quantitatively different from that of type I fibers. That is, although type

II terminals have clear, round vesicles, they are on average smaller (46.3 ± 4.6 μm in diameter) than those of type I fibers, and much of their membrane apposition is synaptic (Fig. 2.18A, arrows). Although the sample size is small, there is a distinct difference in the size of the postsynaptic plaque compared to the extent of membrane apposition for synapses of the two types of auditory nerve fibers: for synapses of type I fibers, this ratio is 6–26%, whereas for synapses of type II fibers the ratio is 42–77% (Ryugo et al. 1991).

There seems to be little question that type I fibers transmit information from IHCs to neurons of the cochlear nucleus. Type II fibers also have a morphology consistent with the capability to convey "sensory" information from OHCs directly to neurons in the cochlear nucleus. Such communication may not necessarily be directly related to the acoustic environment but rather pertain to the functional status of the OHCs, perhaps providing feedback to the brain analogous to muscle spindle afferents. This idea, however, would not preclude OHCs from participating in mechanisms that determined the responses of IHCs, and influencing the information carried by type I fibers. Nor would it preclude the possibility that both sets of afferents might synaptically converge on the same neurons in the cochlear nucleus. What is needed is a clarification of the response characteristics and central connections of the type II ganglion cells.

4.2.8 Central Projections in Humans

We have very few details concerning the central projections of the auditory nerve in humans. Information has been limited due to the obvious ethical and philosophical considerations, coupled with technological constraints in studying postmortem material. The thickness of the auditory nerve ranges from 1.15–2.62 mm with a mean (± S.D.) of 1.76 ± 0.53 (Natout et al. 1987). Cochlear nerve fibers range in diameter from 3–11 μm with more than half in the 3–5 μm range; no mention has been made of the unmyelinated fibers (Natout et al. 1987). Presently, however, there are methods to study the central projections of single fibers in postmortem tissue. In formalin-fixed tissue, HRP (Kageyama and Meyer 1987; Haber 1988) and carbocyanine dyes (e.g., Godement et al. 1987) have been successfully applied to study neurons and fiber pathways. The fluorescent carbocyanine dyes can be stabilized using a photoconversion procedure (McConnell, Ghosh, and Shatz 1989). These methods open up whole new vistas for neuroanatomical research in the human nervous system.

5. Summary

No description of the auditory nerve can be considered complete until we have much greater knowledge of the details of synaptic connections between primary afferents, peripheral receptors, and neuron classes in the brain. Considerable information is waiting to be gathered. Such a description is necessary if we are to understand the structural basis by which neural activity from the auditory nerve is "processsed" by the cochlear nucleus, because the coding process is hypothesized to be influenced by definable features of the relationship between pre- and postsynaptic cells. We still need to know the specific locations (i.e., cell body, proximal or distal dendrite, axon hillock) that certain terminal types (from type I or type II fibers) make on identifiable cells.

Nevertheless, at this time it still seems safe to propose that the connections between the cochlea and the cochlear nucleus are represented by two separate systems, both of which have the apparatus for chemical transmission in the central nervous system (Fig. 2.19). There is one system for the rapid conduction of auditory information which arises from a punctate region of the basilar membrane and is conveyed by IHCs and the myelinated axons of type I neurons. A parallel system arises from a length of basilar membrane and utilizes OHCs and the unmyelinated axons of type II neurons. Afferent information from both types of hair cell receptors can apparently influence widely separate regions within the cochlear nucleus, but the effective stimulus, the latency to activation, and the neuronal targets appear to be profoundly different.

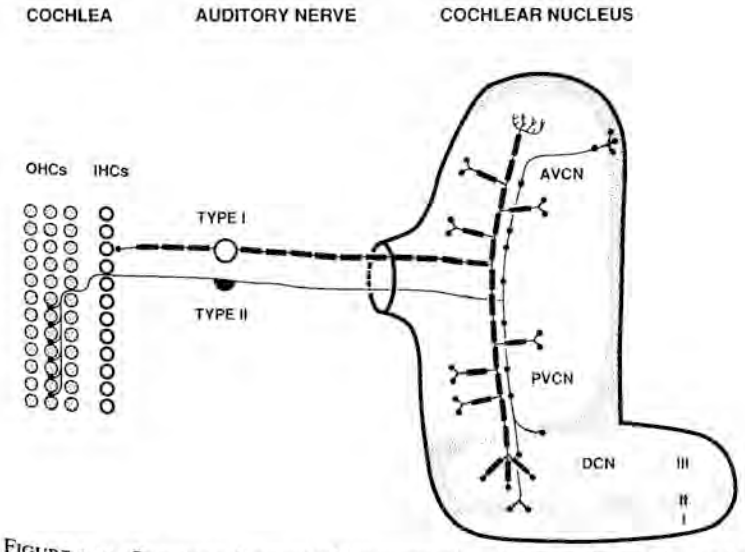

FIGURE 2.19. Summary diagram of the connections between the cochlea and the cochlear nucleus. Two separate but parallel systems convey information from the acoustic receptors to the brain.

Acknowledgements. The author was supported by NIH grant R01 DC00232 during the preparation of this chapter. Special thanks to Tan Pongstaporn and Debora D. Wright for technical assistance, and to Dr. R.S. Kimura for providing micrographs used in Figures 2.1 and 2.2.

References

Adams JC (1983) Cytology of periolivary cells and the organization of their projections. J Comp Neurol 215:275–289.

Alving BM, Cowan WM (1971) Some quantitative observations on the cochlear division of the eighth nerve in the squirrel monkey (*Saimiri sciureus*). Brain Res 25:229–239.

Anniko M, Arnesen AR (1988) Cochlear nerve topography and fiber spectrum in the pigmented mouse. Arch Otorhinolaryngol 245:155–159.

Arnesen AE, Osen KK (1978) The cochlear nerve in the cat: Topography, cochleotopy, and fiber spectrum. J Comp Neurol 178:661–678.

Arnesen AE, Osen KK, Mugnaini E (1978) Temporal and spatial sequence of anterograde degeneration in the cochlear nerve fibers of the cat. A light microscopic study. J Comp Neurol 178:679–696.

Berglund AM, Brown MC (1989) Axonal trajectories of type-II spiral ganglion cells from various cochlear regions in mice. Soc Neurosci Abstr 15:742.

Berglund AM, Ryugo DK (1986) A monoclonal antibody labels type II cells of the spiral ganglion. Brain Res 383:327–332.

Berglund AM, Ryugo DK (1987) Hair cell innervation by spiral ganglion neurons in the mouse. J Comp Neurol 255:560–570.

Berglund AM, Ryugo DK (1991) Neurofilament antibodies and spiral ganglion neurons of the mammalian cochlea. J Comp Neurol (in press).

Bohne BA, Kenworthy A, Carr CD (1982) Density of myelinated nerve fibers in the chinchilla cochlea. J Acoust Soc Am 72:102–107.

Borg E (1972) Acoustic middle ear reflexes: A sensory-control system. Acta Otolaryngol (Stockh) Suppl 304:1–34.

Borg E (1973) On the neuronal organization of the acoustic middle ear reflex. A physiological and anatomical study. Brain Res 49:101–123.

Bourk TR, Mielcarz JP, Norris BE (1981) Tonotopic organization of the anteroventral cochlear nucleus of the cat. Hear Res 4:215–241.

Brawer JR, Morest DK (1975) Relations between auditory nerve endings and cell types in the cat's anteroventral cochlear nucleus seen with the Golgi method and Nomarski optics. J Comp Neurol 160:491–506.

Brawer JR, Morest DK, Kane EC (1974) The neuronal architecture of the cochlear nucleus of the cat. J Comp Neurol 155:251–300.

Bredberg G (1968) Cellular pattern and nerve supply of the human organ of Corti. Acta Otolaryngol (Suppl 236) 1–135.

Brown MC (1987a) Morphology of labeled afferent fibers in the guinea pig cochlea. J Comp Neurol 260:591–604.

Brown MC (1987b) Morphology of labeled efferent fibers in the guinea pig cochlea. J Comp Neurol 260:591–604.

Brown MC, Berglund, AM, Kiang NYS, Ryugo DK (1988a) Central trajectories of type II spiral ganglion neurons. J Comp Neurol 278:581–590.

Brown MC, Ledwith JV (1990) Projections of thin (type-II) and thick (type-I) auditory-nerve fibers into the cochlear nucleus of the mouse. Hear Res 49:105–118.

Brown MC, Liberman MC, Benson TE, Ryugo DK (1988b) Brainstem branches from olivocochlear axons in cats and rodents. J Comp Neurol 278:591–603.

Brown MC, Nuttall AL (1984) Efferent control of cochlear inner hair cell responses in the guinea-pig. J Physiol (Lond) 354:625–646.

Bruns V, Schmieszek E (1980) Cochlear innervation in the greater horseshoe bat: Demonstration of an acoustic fovea. Hear Res 3:27–43.

Burda H (1984) Guinea pig cochlear hair cell density; Its relation to frequency discrimination. Brain Res 14:315–317.

Cant NB, Morest DK (1979) The bushy cells in the anteroventral cochlear nucleus of the cat. A study with the electron microscope. Neuroscience 4:1925–1945.

Cohen ES (1972) Synaptic Organization of the Caudal Cochlear Nucleus of the Cat. Doctoral Thesis, Harvard University, Cambridge, MA.

Covey E, Jones DR, Casseday JH (1984) Projections from the superior olivary complex to the cochlear nucleus in the tree shrew. J Comp Neurol 226:289–305.

Dallos P (1971) On the limitations of cochlear microphonic measurements. J Acoust Soc Am 49:1141–1154.

Dunn RA (1975) A comparison of Golgi-impregnated innervation patterns and fine structural synaptic morphology in the cochlea of the cat. Doctoral Thesis, Harvard University, Cambridge, MA.

Ehret G (1979) Quantitative analysis of nerve fibre densities in the cochlea of the house mouse (*Mus musculus*). J Comp Neurol 193:73–88.

Ehret G (1983) Peripheral anatomy and physiology II. In: Willott JF (ed) The Auditory Psychobiology of the Mouse. Springfield, IL: Charles C Thomas, pp. 169–200.

Ehret G, Frankenreiter M (1977) Quantitative analysis of cochlear structures in the house mouse in relation to mechanisms of acoustic information processing. J Comp Physiol 122:65–85.

Engström H, Wersäll J (1958) Structure and innervation of the inner ear sensory epithelia. Int Rev Cytol 7:535–585.

Evans EF (1972) The frequency response and other properties of single fibres in the guinea-pig cochlear nerve. J Physiol 226:263–287.

Evans EF, Palmer AR (1980) Relationship between the dynamic range of cochlear nerve fibers and their spontaneous activity. Exp Brain Res 40:115–118.

Fay RR (1988) Hearing in Vertebrates. Winnetka, IL: Hill-Fay Associates.

Fekete DM, Rouiller EM, Liberman MC, Ryugo DK (1984) The central projections of intracellularly labeled auditory nerve fibers in cats. J Comp Neurol 229:432–450.

Feldman ML, Harrison JM (1969) The projection of the acoustic nerve to the ventral cochlear nucleus of the rat. A Golgi study. J Comp Neurol 137:267–294.

Firbas W (1972) Uber anatomische Anpassungen des Hörogans an die Aufnahme hoher Frequenzen. Mschr Ohr hk Laryngol-Rhinol (Vienna) 106:105–156.

Gacek RR, Rasmussen GL (1961) Fiber analysis of the statoacoustic nerve of guinea pig, cat and monkey. Anat Rec 139:455–463.

Gambetti P, Antilio-Gambetti L, Papasozomenos S (1982) Bodian's silver method stains neurofilament polypeptides. Science 213:1521–1522.

Gentschev T, Sotelo C (1973) Degenerative patterns in the ventral cochlear nucleus of the rat after primary deafferentation. An ultrastructural study. Brain Res 62:37–60.
Gifford ML, Guinan JJ (1987) Effects of electrical stimulation of medial olivocochlear neurons on ipsilateral and contralateral cochlear responses. Hear Res 29:179–194.
Ginzberg RD, Morest DK (1983) A study of cochlear innervation in the young cat with the Golgi method. Hearing Res 10:227–246.
Godement P, Vanselow J, Thanos S, Bonhoeffer F (1987) A study in developing visual systems with a new method of staining neurones and their processes in fixed tissue. Development 101:697–713.
Godfrey, DA, Kiang NYS, Norris BE (1975) Single unit activity in the posteroventral cochlear nucleus of the cat. J Comp Neurol 162:247–268.
Gray EG, Guillery RW (1966) Synaptic morphology in the normal and degenerating nervous system. Int Rev Cytol 19:111–182.
Guild SR, Crowe SJ, Bunch CC, Polvogt LM (1931) Correlations of differences in the density of innervation of the organ of Corti with differences in the acuity of hearing, including evidence as to the location in the human cochlea of the receptors for certain tones. Acta Otolaryngol (Stockh) 15:269–308.
Guinan JJ, Warr WB, Norris BE (1983) Differential olivocochlear projections from lateral vs medial zones of the superior olivary complex. J Comp Neurol 221:358–370.
Haber S (1988) Tracing intrinsic fiber connections in postmortem human brain with WGA-HRP. J Neurosci Methods 23:15–22.
Harrison JM, Irving R (1966) Ascending connections of the anterior ventral cochlear nucleus in the rat. J Comp Neurol 126:51–64.
Held H (1926) Die Cochlea der Säuger und der Vögel, ihre Entwicklung und ihr Bau. In: Bethe A, v Bergman G, Ellinger A (ed) Handbuch der Normalen und Pathologischen Physiologie, Vol. XI. Berlin: J Springer, pp. 467–534.
Ibata Y, Pappas GD (1976) The fine structure of synapses in relation to the large spherical neurons in the anterior ventral cochlear (sic) of the cat. J Neurocytol 5:395–406.
Innocenti GM, Fiori L, Caminiti R (1977) Exuberant projection into the corpus callosum from the visual cortex of newborn cats. Neurosci Lett 4:237–242.
Irving R, Harrison JM (1967) The superior olivary complex and audition: A comparative study. J Comp Neurol 130:77–86.
Ishii D, Balough Jr. K (1968) Distribution of efferent nerve endings in the organ of Corti. Their graphic reconstruction in cochleae by localization of acetylcholinasterase activity. Acta Otolaryngol 66:282–288.
Jackson H, Parks TN (1982) Functional synapse elimination in the developing avian cochlear nucleus with simultaneous reduction in cochlear nerve axon branching. J Neurosci 2:1736–1743.
Johnstone BM, Pattuzzi R, Yates GK (1986) Basilar membrane measurements and the traveling wave. Hear Res 22:147–153.
Kageyama GH, Meyer RL (1987) Dense HRP filling in pre-fixed brain tissue for light and electron microscopy. J Histochem Cytochem 35:1127–1136.
Kawase K, Liberman MC (1991) Spatial organization of the spiral ganglion according to spontaneous discharge rate. Assn Res Otolaryngol Abst p. 17.
Keithley EM, Feldman ML (1979) Spiral ganglion cell counts in an age-graded series of rat cochleas. J Comp Neurol 188:429–442.

Keithley EM, Feldman ML (1982) Hair cell counts in an age-graded series of rat cochleas. Hear Res 8:249–262.
Keithley EM, Feldman ML (1983) The spiral ganglion and hair cells of the Bronx waltzer mice. Hear Res 12:381–391.
Keithley EM, Schreiber RC (1987) Frequency map of the spiral ganglion in the cat. J Acoust Soc Am 81:1036–1042.
Kellerhals B, Engström H, Ades HW (1967) Die Morphologie des Ganglion spirale Cochleae. Acta Otolaryngol Supp 226:6–33.
Khanna SM, Leonard DGB (1982) Basilar membrane tuning in the cat cochlea. Science 215:305–306.
Kiang NYS, Watanabe T, Thomas LC, Clark LF (1965) Discharge Patterns of Single Fibers in the Cats Auditory Nerve. Cambridge: MIT Press.
Kiang NYS, Rho JM, Northup CC, Liberman MC, Ryugo DK (1982) Hair-cell innervation by spiral ganglion cells in adult cats. Science 217:175–177.
Kiang NYS, Keithley EM, Liberman MC (1983) The impact of auditory nerve experiments on cochlear implant design. Ann NY Acad Sci 405:114–121.
Kiang NYS, Liberman MC, Gage JS, Northrup CC, Dodds LW, Oliver ME (1984) Afferent innervation of the mammalian cochlea. In: Bolis L, Keynes RD, Maddrell HP (eds) Comparative Physiology of Sensory Systems. Cambridge: Cambridge University Press, pp. 143–161.
Kiang NYS, Liberman MC, Sewell WF, Guinan JJ (1986) Single unit clues to cochlear mechanisms. Hear Res 22:171–182.
Kim DO, Molnar CE (1979) A population study of cochlear nerve fibres: Comparison of spatial distributions of average rate and phase-locking measures of responses to single tones. J Neurophysiol 42:16–30.
Kimura RS (1975) The ultrastructure of the organ of Corti. Int Rev Cytol 42:173–222.
Kimura RS (1986) An electron microscopic study of cochlear nerve fibers followed serially from spiral ganglion to organ of Corti. Ear Res Jpn 17:4–7.
Kimura RS, Bongiorno CL, Iverson NA (1987) Synapses and ephapses in the spiral ganglion. Acta Otolaryngol Suppl 438:3–18.
Kohllöffel LUE (1975) A study of neurone activity in the spiral ganglion of the cat's basal turn. Arch Oto Rhino Laryngol 209:179–202.
Leake PA, Snyder RL (1989) Topographic organization of the central projections of the spiral ganglion in cats. J Comp Neurol 281:612–629.
Lenn NY, Reese TS (1966) The fine structure of nerve endings in the nucleus of the trapezoid body and the ventral cochlear nucleus. Am J Anat 118:375–389.
Liberman MC (1978) Auditory-nerve response from cats raised in a low-noise chamber. J Acoust Soc Am 53:442–455.
Liberman MC (1980a) Morphological differences among radial afferent fibers in the cat cochlea: An electron microscopic study of serial sections. Hear Res 3:45–63.
Liberman MC (1980b) Efferent synapses in the inner hair cell area of the cat cochlea: An electron microscopic study of serial sections. Hear Res 3:189–204.
Liberman MC (1982a) Single-neuron labeling in the cat auditory nerve. Science 216:1239–1241.
Liberman MC (1982b) The cochlear frequency map for the cat: Labelling auditory-nerve fibers of known characteristic frequency. J Acoust Soc Am 72:1441–1449.
Liberman MC (1990) Effects of chronic cochlear de-efferentation on auditory-nerve response. Hear Res 49:209–224.

Liberman MC, Kiang NYS (1978) Acoustic trauma in cats: Cochlear pathology and auditory-nerve activity. Acta Otolaryngol Suppl 358:1–63.
Liberman MC, Kiang NYS (1984) Single-neuron labeling and chronic cochlear pathology. Stereocilia damage and alterations in rate- and phase-level functions. Hear Res 16:75–90.
Liberman MC, Oliver ME (1984) Morphometry of intracellular labeled neurons of the auditory nerve: Correlations with functional properties. J Comp Neurol 223:163–176.
Liberman MC, Dodds LW, Pierce S (1990) Afferent and efferent innervation of the cat cochlea: Quantitative analysis with light and electron microscopy. J Comp Neurol 301:443–460.
Lorente de Nó R (1933) Anatomy of the eighth nerve. III. General plan of structure of the primary cochlear nuclei. Laryngoscope 43:327–350.
Lorente de Nó R (1937) The sensory endings in the cochlea. Laryngoscope (St. Louis) 47:373–377.
Masterton RB, Thompson GC, Bechtold JK, RoBards MJ (1975) Neuroanatomical basis of binaural phase-difference analysis for sound localization: A comparative study. J Comp Physiol Psych 89:379–386.
McConnell SK, Ghosh A, Shatz CJ (1989) Subplate neurons pioneer the first axon pathway for the cerebral cortex. Science 245:978–982.
Morrison D, Schindler RA, Wersäll J (1975) A quantitative analysis of the afferent innervation of the organ of Corti in guinea pig. Acta Otolaryngol 79:11–23.
Moskowitz N, Liu JC (1972) Central projections of the spiral ganglion of the squirrel monkey. J Comp Neurol 144:335–344.
Munzer FT (1931) Uber markhaltige Ganglienzellen. Z Mikrosk Anat Forsch 24:286–361.
Nadol JB (1981) Reciprocal synapses at the base of outer hair cells in the organ of Corti of man. Ann Oto Rhinol Laryngol 90:12–17.
Nadol JB (1983a) Serial section reconstruction of the neural poles of hair cells in the human organ of Corti. I. Inner hair cells. Laryngoscope 93:599–614.
Nadol JB (1983b) Serial section reconstruction of the neural poles of hair cells in the human organ of Corti. II. Outer hair cells. Laryngoscope 93:780–791.
Nadol JB (1988a) Comparative anatomy of the cochlea and auditory nerve in mammals. Hear Res 34:253–266.
Nadol JB (1988b) Innervation densities of inner and outer hair cells of the human organ of Corti. ORL 50:363–370.
Natout MAY, Terr LI, Linthicum Jr FH, House WF (1987) Topography of vestibulocochlear nerve fibers in the posterior cranial fossa. Laryngoscope 97:954–958.
Noda Y, Pirsig W (1974) Anatomical projection of the cochlea to the cochlear nuclei of the guinea pig. Arch Otorhinolaryngol 208:107–120.
Osen KK (1969) Cytoarchitecture of the cochlear nuclei in the cat. J Comp Neurol 136:453–484.
Osen KK (1970) Course and termination of the primary afferents in the cochlear nuclei of the cat. Arch Ital Biol 108:21–51.
Ota CY, Kimura RS (1980) Ultrastructural study of the human spiral ganglion. Acta Otolaryngol 89:53–62.
Perkins RE, Morest DK (1975) A study of cochlear innervation patterns in cats and rats with the Golgi method and Nomarski optics. J Comp Neurol 63:129–158.

Polyak SL, McHugh G, Judd DK (1946) The Human Ear in Anatomical Transparencies. Elmsford, NY: Sonotone.
Ramón-Moliner E (1970) The Golgi-Cox technique. In: Nauta WJH, Ebbesson SOE (eds) Contemporary Research Methods in Neuroanatomy. New York, NY: Springer-Verlag, pp. 32–55.
Ramón y Cajal S (1909) Histologie du Système nerveux de l'Homme et des Vertébrés, Vol 1. Madrid: Instituto Ramón y Cajal, pp. 774–838.
Ramprashad F, Money KE, Landolt JP, Laufer J (1978) A neuroanatomical study of the cochlea of the little brown bat (*Myotis lucifugus*). J Comp Neurol 178:347–363.
Ramprashad F, Landolt JP, Money KE, Clark D, Laufer J (1979) A morphometric study of the cochlea of the little brown bat (Myotis lucifugus) J Morphol 160:345–368.
Rasmussen GL (1940) Studies of the VIIIth cranial nerve of man. Laryngoscope 50:67–83.
Rasmussen GL (1946) The olivary peduncle and other fiber connections of the superior olivary complex. J Comp Neurol 84:141–219.
Retzius G (1884) Das Gehörorgan der Wirbeltiere. II. Das Gehörorgan der Reptilien, derr Vögel und der Säugetiere. Stockholm: Samson and Wallin.
Retzius G (1892) Die Endigungsweise des Gehörnerven. Biolog Untersuchungen, Neue Folfe, III. Leipzig: Vogel.
Rhode WS (1971) Observations of the vibration of the basilar membrane in squirrel monkeys using the Mössbauer technique. J Acoust Soc Am 49:1218–1231.
Rhode WS, Oertel D, Smith PH (1983) Physiological response properties of cells labeled intracellularly with horseradish peroxidase in cat ventral cochlear nucleus. J Comp Neurol 213:448–463.
Ritz LA, Brownell WE (1982) Single unit analysis of the posteroventral cochlear nucleus of the decerebrate cat. Neuroscience 7:1995–2010.
Robertson D (1984) Horseradish peroxidase injection of physiologically characterized afferent and efferent neurons in the guinea pig spiral ganglion. Hear Res 15:113–121.
Robertson D, Cody AR, Bredberg G, Johnstone BM (1980) Response properties of spiral ganglion neurons in cochleas damaged by direct mechanical trauma. J Acoust Soc Am 67:1295–1303.
Romand R, Hafidi A, Despres G (1987) Immunocytochemical localization of neurofilament protein subunits in the spiral ganglion of the adult rat. Brain Res 462:167–173.
Rose JE, Galambos R, Hughes JR (1959) Microelectrode studies of the cochlear nuclei of the cat. Bull Johns Hopkins Hospital 104:211–251.
Rouiller EM, Cronin-Schreiber R, Fekete DM, Ryugo DK (1986) The central projections of intracellularly labeled auditory nerve fibers in cats: An analysis of terminal morphology. J Comp Neurol 249:261–278.
Rouiller EM, Ryugo DK (1984) Intracellular marking of physiologically characterized neurons in the ventral cochlear nucleus of the cat. J Comp Neurol 225:167–186.
Russel IJ, Sellick PM (1978) Intracellular studies of hair cells in the mammalian cochlea. J Physiol 284:261–290.
Ryan AF, Schwartz IR, Helfert RH, Keithley EM, Wang ZX (1987) Selective retrograde labeling of lateral olivocochlear neurons in the brainstem based on

preferential uptake of ^{3}H-D-aspartic acid in the cochlea. J Comp Neurol 255:606–616.
Ryugo DK, Fekete DM (1982) Morphology of primary axosomatic endings in the anteroventral cochlear nucleus of the cat: A study of the endbulbs of Held. J Comp Neurol 210:239–257.
Ryugo DK, Rouiller EM (1988) The central projections of intracellularly labeled auditory nerve fibers in cats: Morphometric correlations with physiological properties. J Comp Neurol 271:130–142.
Ryugo DK, Sento S (1991) Synaptic connections of the auditory nerve in cats: Relationship between endbulbs of Held and spherical bushy cells. J Comp Neurol 305:35–48.
Ryugo DK, Dodds LW, Benson TE, Kiang NYS (1991) Unmyelinated axons of the auditory nerve in cats. J Comp Neurol (in press).
Sachs MB, Abbas PJ (1974) Rate versus level functions for auditory nerve fibers in cats: Tone-burst stimulation. J Acoust Soc Am 56:1835–1847.
Sando I (1965) The anatomical interrelationships of the cochlear nerve fibers. Acta Otolaryngol 59:417–436.
Schalk TB, Sachs MB (1980) Nonlinearities in auditory-nerve fiber responses to bandlimited noise. J Acoust Soc Am 67:903–913.
Schuknecht HF (1953) Techniques for study of cochlear function and pathology in experimental animals. Arch Oto-Laryngol 58:377–397.
Schuknecht HF (1960) Neuroanatomical correlates of auditory sensitivity and pitch discrimination in the cat. In: Rasmussen GL, Windle WF (eds) Neural Mechanisms of the Auditory and Vestibular Systems. Springfield, IL: Charles C Thomas, pp. 76–90.
Sento S, Ryugo DK (1989) Endbulbs of Held and spherical bushy cells in cats: Morphological correlates with physiological properties. J Comp Neurol 280:553–562.
Simmons DD, Liberman MC (1988) Afferent innervation of outer hair cells in adult cats: I. Light microscopic analysis of fibers labeled with horseradish peroxidase. J Comp Neurol 270:132–144.
Smith CA (1961) Innervation pattern of the cochlea. The internal hair cell. Ann Otol Rhinol Laryngol 70:1–24.
Smith CA (1975) Innervation of the cochlea of the guinea pig by use of the Golgi stain. Ann Otol Rhinol Laryngol 84:443–458.
Smith CA, Rasmussen GL (1963) Recent observation on the olivocochlear bundle. Ann Otol Rhinol Laryngol 72:489–497.
Smith CA, Sjöstrand FS (1961) Structure of the nerve endings on the external hair cells of the guinea pig cochlea as studied by serial section. J Ultrastruct Res 5:523–556.
Spangler KM, Cant NB, Henkel CK, Farley GR, Warr WB (1987) Descending projections from the superior olivary complex to the cochlear nucleus of the cat. J Comp Neurol 259:452–465.
Spirou GA, May BJ, Ryugo DK (1989) 3-Dimensional frequency mapping in the cat dorsal cochlear nucleus. Soc Neurosci Abst 15:744.
Spoendlin H (1969) Innervation patterns in the organ of Corti of the cat. Acta Otolaryngol (Stockh) 67:239–254.
Spoendlin H (1971) Degeneration behavior of the cochlear nerve. Arch Klin Exp Ohr- Nas- Kehlk Heilk 200:275–291.

Spoendlin H (1972) Innervation densities of the cochlea. Acta Otolaryngol 73:235–248.
Spoendlin H (1973) The innervation of the cochlea receptor. In: Moller AR (ed) Mechanisms in Hearing. New York: Academic Press, pp. 185–229.
Spoendlin H (1975) Retrograde degeneration of the cochlear nerve. Acta Otolaryngol 79:266–275.
Spoendlin H (1979) Neural connections of the outer hair cell system. Acta Otolaryngol 87:381–387.
Spoendlin H (1981) Differentiation of cochlear afferent neurons. Acta Otolaryngol 91:451–456.
Spoendlin H (1982) The innervation of the outer hair cell system. Am J Otol 3:274–278.
Spoendlin H, Schrott A (1988) The spiral ganglion and the innervation of the human organ of Corti. Acta Otolaryngol (Stockh) 105:403–410.
Stanfield BB, O'Leary DDM (1985) The transient corticospinal projections from the occipital cortex during the postnatal development of the rat. J Comp Neurol 238:236–248.
Suzuki Y, Watanabe A, Osada M (1963) Cytological and electron microscopic studies on the spiral ganglion cells of adult guinea pigs and rabbits. Arch Histol Jap 24:9–33.
Tolbert LP, Morest DK (1982) The neuronal architecture of the anteroventral cochlear nucleus of the cat in the region of the cochlear nerve root: Electron microscopy. Neuroscience 7:3053–3067.
Valverde F (1970) The Golgi method: A tool for comparative structural analyses. In: Nauta WJH, Ebbesson SOE (eds) Contemporary Research Methods in Neuroanatomy. New York: Springer-Verlag, pp. 12–31.
von Ebner B (1903) Die Endigung des Schneckennerven im Cortischen Organe. Kölliker's Handbuch der Gewebelehre des Menschen, III. Leipzig: Engelmann, pp. 944–960.
Warr WB (1975) Olivocochlear and vestibular efferent neurons of the feline brainstem: Their location, morphology, and number determined by retrograde axonal transport and acetylcholinesterase histochemistry. J Comp Neurol 161:159–182.
Warr WB, Guinan JJ (1979) Efferent innervation of the organ of Corti: Two separate systems. Brain Res 173:152–155.
Webster DB (1971) Projection of the cochlea to cochlear nuclei in Merriam's kangaroo rat. J Comp Neurol 143:323–340.
White JS, Warr WB (1983) The dual origins of the olivocochlear bundle in the albino rat. J Comp Neurol 219:203–214.
Wiederhold ML (1970) Variations in the effects of electrical stimulation of the crossed olivocochlear bundle on cat single auditory-nerve-fiber responses to tone bursts. J Acoust Soc Am 48:966–977.
Wiederhold ML, Kiang NYS (1970) Effects of electric stimulation of the crossed olivocochlear bundle on single auditory-nerve fibers in the cat. J Acoust Soc Am 48:950–965.
Wright DD, Spirou GA, May BJ, Ryugo DK (1991) Frequency representation in the dorsal cochlear nucleus of cats. Assn Res Otolaryngol Abst p. 140.